

MODELLING AND ANALYSIS OF CNC TURNING PROCESS

**A Thesis Submitted
in Partial Fulfillment of the Requirements
for the Degree of**

MASTER OF TECHNOLOGY

in

DESIGN ENGINEERING

by

Mohd Aseerullah

(1200456003)

Under the Supervision of

Mr. Chandra Bhushan

Asst. Professor

Department of Mechanical Engineering

Babu Banarsi Das University, Lucknow



BBD UNIVERSITY

**to the
School of Engineering**

**BABU BANARASI DAS UNIVERSITY
LUCKNOW**

June, 2022

CERTIFICATE

It is certified that the work contained in this thesis entitled " Modelling and Analysis of CNC Turning Process by Mohd Aseerullah (1200456003), for the award of Master of Technology from Babu Banarasi Das University has been carried out under my/our supervision and that this work has not been submitted elsewhere for a degree.

Signature

(Mr. Chandra Bhushan)

(Assistant Professor)

(Department of Mechanical Engineering)

(BBDU-Lucknow)

Date:

MODELLING AND ANALYSIS OF CNC TURNING PROCESS

Mohd Aseerullah

ABSTRACT

In this new technological world, CNC and manual turning operations engage in a significant role in different types of designing and manufacturing industries. Before initiating the manufacturing processes, analysis is a crucial part of the manufacturing process. This study involves modelling and analysis of the CNC machining process of a cylindrical AA6082-T6 workpiece with a Tungsten Carbide tip tool. A 3D model is first modelled on CATIA V5 and the analysis is then carried on in Ansys R19.2's explicit module. The experimental and analytical results are carried out to justify the work. The cutting parameters used in CNC machining are Spindle rotational speed, feed rate, and depth of cut. By FEA analysis the values of the stresses and the strains are calculated and then compared to the analytical results that was calculated by the help of the experimental values we get by performing the experiment on a CNC machine. The CNC machine employed is Siemens Sinumerik 828D. When the experiment was carried out the cutting specifications used during CNC machining are spindle rotational speed, feed rate, and depth of cut. The percentage error value for Normal Stress differed too much already when compared to Shear Stress and Shear Strain. This demonstrates that aluminum is best suited for machining operations and that it could also be used more effectively.

ACKNOWLEDGEMENT

My Head bows with reverence before the almighty God, and my Father Mr. Mohd Dawood who has given me strength, wisdom and will to complete the work.

It is a great pleasure to express my great sincere gratitude and profound regards to Assistant Professor Mr. Chandra Bhushan for his constant encouragement, invaluable guidance and help during the course of work. Words are inadequate to acknowledge the care and keen interest taken in all aspect of the present work. I am also Thankful to faculty and staff members of the Mechanical Engineering Department.

I cannot forget to give special thanks to my friends. This work, which is significant work of my career, could not have been attempted without the understanding, patience and assistance of my parents, my gratitude to them is profound.

Mohd Aseerullah

Table of Contents

CERTIFICATE	ii
ABSTRACT.....	iii
ACKNOWLEDGEMENT	iv
Table of Contents	v
List of Tables.....	viii
List of Figures	ix
List of Symbols, abbreviations and Nomenclature	xi
1 INTRODUCTION	1
1.1 BACKGROUND	1
1.2 CNC Turning	2
1.3 Software Used	3
1.3.1 CATIA V5.....	3
1.3.2 Ansys R19.2	3
1.4 PARAMETRIC MODELLING	4
1.5 LITERATURE REVIEW	5
1.6 RESEARCH OBJECTIVE	7
1.7 THESIS OUTLINE	7
2 WORKPIECE & TOOL MODELLING	8
2.1 Geometric Model of Physical Simulation	8
2.2 Modelling of the Workpiece	9
2.3 Modelling of the Tool	10
2.4 Tool and Workpiece Used	11
2.5 Saving & Importing the Model for Analysis	13
3 PROPERTIES OF MATERIALS USED	15
3.1 General Properties	15
3.2 Properties of the Workpiece Used.....	16
3.2.1 Chemical Composition of the Workpiece	17
3.2.2 Mechanical Properties of the Workpiece	18
3.2.3 Failure Model of the Workpiece	18
3.3 Properties of the Tool Used	19
4 CONNECTIONS AND MESHING.....	21

4.1	Coordinate System	21
4.1.1	Global Coordinate System.....	21
4.1.2	Cylindrical Coordinate System	22
4.2	Connections.....	24
4.2.1	Contacts.....	24
4.2.2	Body Interaction.....	26
4.3	Meshing.....	27
4.3.1	Size of Mesh	29
4.3.2	Quality of the Mesh.....	30
4.3.3	Statistics of Mesh	31
5	BOUNDARY CONDITIONS & ANALYSIS SETTINGS.....	32
5.1	Boundary Conditions.....	32
5.1.1	Initial Conditions	33
5.1.2	Displacement to the Workpiece	33
5.1.3	Displacement to the Tool.....	35
5.2	Analysis Settings.....	37
5.2.1	Step Controls.....	38
5.2.2	Solver Controls	39
5.2.3	Euler Domain Controls	39
5.2.4	Damping Controls.....	40
5.2.5	Erosion Controls	41
5.2.6	Output Controls.....	42
6	PERFORMING THE EXPERIMENT	43
6.1	Strategy	43
6.1.1	Apparatus Used.....	43
6.1.2	CNC Machine Used.....	44
6.1.3	Measuring Device Used.....	46
6.1.4	Part Program Used	46
6.1.5	Performing the Turning Process.....	49
6.2	Final Product	53
7	RESULT & JUSTIFICATION	55
7.1	FEA Results	55
7.2	Experimental Results.....	60
7.3	Analytical Results	61
8	CONCLUSION & FUTURE WORK	65

8.1	Conclusion	65
8.2	Future Work	66
REFERENCES		67
List of Publications		71

List of Tables

Table 3.1 Chemical Composition(wt.%) of AA6082-T6	18
Table 3.2 Mechanical Properties of the Workpiece	18
Table 3.3 Failure Properties of the Workpiece	19
Table 3.4 Mechanical Properties of the Tool	20

List of Figures

Figure 1.1 Turning Process	2
Figure 1.2 Logo of CATIA software.....	3
Figure 1.3 Logo of Ansys Software	4
Figure 2.1 A 3-D geometric model of an insert cutting a workpiece in turning.	9
Figure 2.2 3D model of the Workpiece.....	10
Figure 2.3 3D model of the Tool.....	11
Figure 2.4 A Cylindrical AA6082-T6 bar	12
Figure 2.5 Carbide Insert Tool.....	12
Figure 2.6 Explicit Dynamics Module Screen of Ansys R19.2 Workbench.....	13
Figure 2.7 Imported Geometry to Ansys R19.2 software	14
Figure 3.1 Quantitative Measurements of Five Material Properties	16
Figure 3.2 Properties view in Engineering Data module of Ansys R19.2	17
Figure 3.3 Properties view in Engineering Data module of Ansys R19.2.....	20
Figure 4.1 Global Coordinate System.....	22
Figure 4.2 Cylindrical Coordinate System.....	23
Figure 4.3 Cylindrical coordinate system with respect to angle	23
Figure 4.4 Scoping Method of Contact	24
Figure 4.5 Contact Body	25
Figure 4.6 Target Body	26
Figure 4.7 Body Interaction	27
Figure 4.8 Meshing of the Workpiece.....	28
Figure 4.9 Meshing of the Tool & the Tool Holder	28
Figure 4.10 Mesh Sizing	29
Figure 4.11 Quality of the Mesh	30
Figure 4.12 Statistics of the Mesh	31
Figure 5.1 Displacement employed on Workpiece	34
Figure 5.2 Details of Displacement employed on the Workpiece.....	35
Figure 5.3 Tabular data of the Displacement of the Workpiece.....	35
Figure 5.4 Displacement employed on Tool.....	36
Figure 5.5 Details of Displacement employed on the Tool and the Tool Holder.....	37
Figure 5.6 Tabular data of the Displacement of the Tool and the Workpiece	37
Figure 5.7 Step Control Options	38
Figure 5.8 Solver Control Options	39
Figure 5.9 Euler Domain Control Options	40
Figure 5.10 Damping Control Options.....	41
Figure 5.11 Erosion Control Options	42
Figure 5.12 Output Control Options	42
Figure 6.1 Siemens Sinumerik 828D Machine	45
Figure 6.2 Specifications of the Machine	45
Figure 6.3 Kistler 9129AA.....	46
Figure 6.4 Stock Removal Cycle	47
Figure 6.5 Workpiece Parameter Input	48
Figure 6.6 Part Program	49

Figure 6.7 Tool moving towards the workpiece	50
Figure 6.8 Tool Cutting the Workpiece	51
Figure 6.9 Tool Moving away from the Workpiece.....	52
Figure 6.10 Chips formed in Turning Process	52
Figure 6.11 The Final Product	53
Figure 6.12 Final Diameter of the Workpiece.....	54
Figure 7.1 Normal Stress Analysis.....	56
Figure 7.2 Line Graph (Time vs Normal Stress).....	57
Figure 7.3 Shear Stress Analysis.....	58
Figure 7.4 Line Graph (Time vs Shear Stress).....	58
Figure 7.5 Shear Strain Analysis.....	59
Figure 7.6 Line Graph (Time vs Shear Elastic Strain).....	60
Figure 7.7 Component Ratio vs Time Graph of Results	61

List of Symbols, abbreviations and Nomenclature

2D:Two Dimension
3D:Three Dimensional
AA:Aluminium Alloy
AISI: American Iron and Steel Institute.
Al:Aluminum
ANOVA: Analysis of variance
C1: Gruneisen Coefficient arameter 1
CAD:Computer Aided Design
CAE:Computer Aided Engineering
CAM:Computer Aided Manufacturing
Catia:Computer Aided three dimensional interactive application
CFL: Courant–Friedrichs–Lewy
CNC: Computer Numerical Control
CPU:Central Processing Unit
Cr: Chromium
Cu: copper
D1:Johnson's First Constant
D2: Johnson's Second Constant
D3: Johnson's third Constant
D4: Johnson's Fourth Constant
D5: Johnson's Fifth Constant
et al.: and others
f:Feed Rate
Fc: Cutting Force Component
Fe: Iron
FEA:Finite Element Analysis
FEM:Finite Element Model
Ff: Feed Force Component
Fr: Radial Force Component
Ft: Thrust Force Component
GUI:Graphical User Interface
i.e.,:that is
ISO: International Organization for Standardization
Mg: Magnesium
mg:miligram
mm:millimeter
Mn: manganese
ms:milliseconds
 ϕ :Shear Angle
PDE:Partial Differential Equation
r:Cutting Ratio
S:Speed Rate

S1: Gruneisen Coefficient Parameter 2
SASI: Swanson Analysis Systems Inc.
Si: Silicon
T:Depth of Cut
TaC: tantalum carbide
Ti: Titanium
TiC: titanium carbide
V5:Version 5
WC:Tungsten Carbide
X:x-axis coordinate
Y: y-axis coordinate
Z: z-axis coordinate
Zn:Zinc
 α :Normal Rake Angle
 α_b :Back Rake Angle
 α_s :Side Rake Angle
 γ :Shear Strain
 σ :Normal Stress
 τ_s :Shear Stress
 Ψ_s :Side Cutting Edge Angle
 Ψ_s : Side Cutting Edge Angle

CHAPTER 1

1 INTRODUCTION

1.1 BACKGROUND

In the manufacturing industry, modeling and analysis play a critical part in assessing product quality. Product quality is the most essential aspect of a product life cycle. Sometimes, Product quality also decides the product life in the market. Quality and consumer satisfaction are the two fundamental goals of any equipment or manufacturing business that every company in the world strives to achieve. Machining is the primary metal processing activity performed on a daily basis in many industrial businesses. Many processing parameters influence the quality of metal cutting obtained, and these process parameters influence the output responsiveness and performance characteristics of the final product to be manufactured. In a conclusion, the primary step in the process of a product's life cycle is the selection of the standard protocol and the proper criterion. Poor process and parameter selection lead to non-optimal machine operation, which can impact tool sharpness and, in some situations, tool and workpiece wear and tear. A cutting tool is used in the metal cutting process to process and remove surplus material from the workpiece in order to transform the workpiece into a desirable part that may subsequently be employed in a variety of activities. The process of creating a high-quality end product at a cheap cost is an important component of a product's life cycle, and it may be accomplished by selecting the appropriate tool material, cutter settings, machine equipment, and tool geometry.

The most significant manufacturing step is machining. Machining is described as the removal of material from a workpiece in the form of chips to gain the desired product as a result. When the material is metallic, the phrase metal cutting is employed. When compared to forming, molding, and casting operations, most machining has a very cheap set-up cost. However, high-volume machining is far more costly. Machining is essential when dimensions and finishes must be held to strict tolerances. The market and procedures in manufacturing sectors are changing very swiftly, therefore to keep pace with the changing in the contemporary world, the optimization of metalworking operations is conducted on several levels to adapt to the new needs in the production unit. In this thesis the modeling and the analysis of the turning process are done with the software explained later in this chapter and the process is an automatic process that is performed on a CNC machine instead of a Lathe machine as nowadays CNC is mostly used for the production in the manufacturing industry.

1.2 CNC Turning

Turning is the technique for removing the outside diameter of a revolving cylindrical workpiece using a single-point cutting tool. Whenever we need to minimize the diameter of a workpiece, particularly within a certain diameter, and also to achieve a smooth surface, we perform a CNC turning or turning operation. When this technique is carried out with the assistance of a computer-based lathe, it is termed a CNC turning operation. To conduct the CNC turning process, the component programmed will be sent to the computer, which accomplishes the operation without the intervention of external labor or very less intervention from the labor. A turret equipped with tooling is programmed to travel to the raw material bar and remove material to produce a desirable outcome. Because it includes material removal, this is also known as "subtraction machining" as it is a type of machining. You cannot avoid shafts in machine construction to transport power from the motor to the moving components. Shafts must be turned. However, CNC turning and drilling are widely used in a variety of sectors to make axis-symmetric components.



Figure 1.1 Turning Process

CNC stands for computer numerical control, which means that automated systems operate the machines. A Digital code is used as input which is known as G-code. This controls all tool motions and spin speed, as well as other supporting operations such as coolant usage. In a CNC Turning process, there are four steps involved. The first step involves creating a digital representation of the part in a CAD (Computer-Aided Design) System. The second step is to create or generate the machining code from the CAD files and this machine code is known as the part program. The third step is to set up the lathe i.e., placing the workpiece and the tool in their respective places for the machining process. The fourth and last step is manufacturing the turned parts and getting the desirable part as the output of the process.

1.3 Software Used

There is two software used in this thesis, one is for creating a 3D model of the system i.e., the tool and the workpiece, and the other one is for the analysis of the system. The software used for creating the 3D model of the system is Catia V5 and the software used for the analysis of the system is Ansys R19.2. This Software is explained in detail in the following section.

1.3.1 CATIA V5

Catia V5 is an acronym that stands for Computer-Aided Three-Dimensional Interactive Application and V5 denotes the version level of the software which is version level 5 of the system in this case. It's much more than just a CAD (Computer-Aided Design) tool. It is also a comprehensive application package that includes many other packages like CAD, CAE (Computer-Aided Engineering), and CAM (Computer-Aided Manufacture). Catia is software developed by a French company named Dassault Systèmes, which currently maintains and develops the software. Dassault Systèmes released CATIA for the first time in the year 1977 it was originally designed to be used in the design of the Dassault Mirage fighter jet and it was developed many times since then.



Figure 1.2 Logo of CATIA software

1.3.2 Ansys R19.2

Ansys, Inc. is an American corporation headquartered in Canonsburg, Pennsylvania. It creates and sells CAE/Multiphysics engineering simulators for product design, product development, testing, and operations, and it serves clients all over the world. John Swanson founded Ansys in 1970. Throughout the 2000s, the company purchased a variety of other design engineering firms, gaining further technologies for fluid dynamics, electronics

development, and physics analysis. Swanson established Ansys in his farmhouse in Pittsburgh under the name Swanson Analysis Systems Inc. (SASI). Swanson produced the very first Ansys software using punch cards and a mainframe computer leased by the hour. Ansys builds and distributes engineering simulation software for utilization across the product's life cycle.

Ansys Mechanical finite element analysis software is used to simulate computer models of structures, electronics, or machine components to analyze their toughness, electromagnetism, elasticity, strength, temperature distribution, fluid flow, and other characteristics. Ansys is used to assess how a product will perform amid diverse conditions without any need for testing equipment or crash testing. Ansys package, for example, may predict how a bridge will hold up after years of activity, how to best process salmon in a cannery to save wastage, or how to build a swing or a slide that uses less material while enhancing safety.



Figure 1.3 Logo of Ansys Software

1.4 PARAMETRIC MODELLING

Parametric modeling is a modeling approach that allows the form of the model geometry to vary as the dimension value changes. To determine the dimension and shape of the model, metric modeling is accomplished using a designed computer programming code such as a script. In CAD systems, during batch modeling, Parametric Modeling techniques play a major role. It may alter or design by changing the parameters' values. Parameters are used to express geometric characteristics and features to relate dimensions with equations and integers in basic parametric modeling. When opposed to the traditional modeling techniques, parametric modeling explicitly establishes relationships among dimensions and limitations. It can help reduce the time and avoid making mistakes regularly.

A commercial CAD System such as Catia is necessary to suit the requirements of the lathe tool parametric modeling. The tool model with parameters may be constructed with custom rules, imported into FEA software, and then results are calculated. The system will then automatically generate an appropriate 3-D model of the lathe tool for FEA computation by adjusting turning parameters such as cutting depth, feed rate, and workpiece diameter.

1.5 LITERATURE REVIEW

Mayur Verma et al. in the year 2019 carried out experimental, analytical, and simulated investigations of CNC turning using various tool inputs. There are numerous alloys in the industry that are extremely difficult to process, necessitating the use of a precise tool, optimal machining settings, tool geometry, and cutting conditions. Resources of various types are vital, difficult, time-consuming, and revenue work for companies in producing the best quality goods at the lowest possible cost to clients. The simulated environment's anticipated characteristics, such as heat, forces, and strain, are confirmed using CNC turning operations utilizing L9 Taguchi orthogonal arrays on Stainless steel AISI 304 with various inserts. Cutting Speed, Feed, and Cutting depth is the CNC turning process parameters used. Any associated analysis may be performed using the verified simulation model. Finite element simulations of CNC turning operations on Stainless steel AISI 304 with various inserts such as Cubic Boron Nitride and Tungsten Carbide inserts are performed in this numerical and experimental study, and the effect of CNC turning process parameters is studied in light of experimental data. Carbide tool inserts and cubic boron nitride tool inserts are the two types of tools employed. Forces are estimated using an analytical study with a workpiece made of aluminum 6061-T6 alloy and an AISI 1045 steel tip tool. The analysis program ANSYS is used to perform numerical research on the orthogonal turning of Aluminum 6061-T6 Alloy with AISI 1045 steel. In the analytical investigation, a workpiece of Aluminum 6061-T6 Alloy is utilized with an AISI 1045 steel tooltip, and forces are determined. To verify the simulated environment, simulated studies for orthogonal, oblique, and cylindrical turning processes are done by using two different combinations, namely aluminum 6061-T6 alloy with AISI 1045 steel tooltip and aluminum 6061-T6 alloy with Tungsten Carbide tooltip to anticipate forces and temperatures. In the experiment, the workpiece is stainless steel AISI 304, and the tool elements are Tungsten Carbide and CBN.

R.K. Bharilya et al. in the year 2015 published a paper in which the trials are conducted using three distinct materials: carburized mild steel, aluminum alloys, and brass. As input, three parameters are provided: spindle speed, depth of cut, and feed rate. When machining hard materials, the depth of cut and feed should be reduced to a minimum, whereas when machining light materials, the depth of cut and feed should then be enhanced since it gives a superior surface finish in the turning process. The purpose of this research is to investigate the optimization of machining parameters for the turning operation of a specific workpiece made of Carburized Mild Steel. Aluminum alloys and brass were manufactured on a CNC machine and tested using a cutting force dynamometer. A dynamometer is a particularly effective piece of machinery for measuring cutting force, and the rotating tool used for precision cutting is constructed of tungsten carbide. The aim is to minimize cutting forces and boost cutting speed in turning operations by utilizing a force dynamometer to optimize process parameters and determine the best surface finish of a specific workpiece. According to our findings, improved surface condition, i.e., surface polish and homogeneity, has been discovered. This might result in lower production costs for elevated CNC machining. The result of this article is that the optimization process for the turning operation with surface quality checks is highly efficient in this technique, with the parameters supplied as T, f, and S. The test results reveal that the optimization report proves the traditionally regarded three control factors (process parameters) such as spindle speed(S), depth of cut(T), and feed

rate(f) that impact material finishing and a wide range of tests for Carburized Mild Steel, Aluminum Alloys, and Brass for surface quality/finishing are optimized.

Magdum Vikas B. et al. in year 2013. In this study, materials for tool and process parameters for forces in turning are chosen for a lot of different aspects. This paper demonstrates a methodology for optimizing cutting forces and other factors. ANOVA and Taguchi orthogonal array are employed for optimizing, and experimentation are carried out to get optimized results, with the outcomes of the trials providing the minimal thrust force. Experiments are carried out in this work to investigate the influence of cutting parameters such as cutting speed, feed rate, and depth of cut on surface roughness during dry turning of 40C8. The goal of this research is to develop multiple regression analyses to gain a better knowledge of the impacts of rotation speed, feed, and cutting depth on surface roughness. For the research setup, a factorial of experiments matching to sessions was used. The contribution of each element to the outcome is determined using an analysis of variance. The feed rate is shown to be the most influential characteristic impacting surface roughness, followed by cutting speed and depth of cut. A number of studies have been carried out in order to begin characterizing the elements influencing surface roughness during the turning process. The influence of rotation speed, flow rate, and cutting depth on 40C8 surface roughness was investigated. The resulting model, which takes into account rotation speed, flow rate, cutting depth, and any two-variable relationships, forecasts surface roughness rather well. The processing parameters tested had a substantial impact on the surface quality of the machined workpiece. Overall, the study finds that feed is the most important element among those evaluated, second by cutting rate and depth of cut. The most important interactions influencing surface roughness of machined surfaces were those between cutting speed and feed.

Dr. Vijay Kumar et al. in year 2017. The influence of lubricating, feed rate, depth of cut, and spindle speed upon EN 19 steel has indeed been explored in this study using L18 Taguchi's orthogonal array, and the relevance of the process variables is assessed using ANOVA. The goal of this study is to cut EN 19 stainless steel material using a CNC turning process and to examine the influencing characteristics while cutting materials, which include surface roughness and material removal rate. The CNC turning process parameters of feed rate, depth of cut, spinning speed/rotational speeds, lubrication, and MRR and surface roughness have already been examined. For the trials, a carbide tip tool was employed as a cutting tool. Taguchi's L18 mixture type orthogonal array experimental design was chosen for inquiry, and optimization is accomplished using Taguchi's technique, as well as analysis of variance (ANOVA) to determine the relevance of process variables on dependent variables. The results show both feed rate and spindle speed have a considerable impact on both material removal rate and surface roughness. The CNC turning study on material removal rates and surface roughness was conducted for EN 19 steel, and the influence of lubricant, feed rate, depth of cut, and speed of rotation on the reaction was investigated under L18. ANOVA is used to examine Taguchi's orthogonal array and the importance of process variables.

1.6 RESEARCH OBJECTIVE

The objectives of this thesis focus on proposing a method of CNC cutting simulation and turning parameters. The work can be concluded by the following aspects:

- Accurate CNC machining tool and workpiece modelling.
- The actual cutting position of the tool and proper meshing in Ansys R19.2 software.
- Accurate FEA results of the CNC turning process.
- To check different parameters of the material in the process by attempting simulations and analyses.
- To check the chip formation and continuity in the process.

1.7 THESIS OUTLINE

This thesis is divided into a total of 8 chapters explaining all the study work and the experimentations involved. Chapter 1 gives a basic idea of the software and the processes used in this thesis. Chapter 2 focuses on the 3D modelling of the tool and the workpiece for the analysis. Chapter 3 is a detailed study of the properties of the tool and the workpiece used in this thesis. Chapter 4 gives us a detailed study about the connections and the type of meshing employed in this thesis. Chapter 5 tells us about the boundary conditions and the analysis settings used in the FEA analysis in the thesis. Chapter 6 gives us the details about performing the experiments involved in this thesis. Chapter 7 shows all the results and the values calculated in this thesis. Chapter 8 gives the conclusion and the future work which can be done later related to this thesis.

CHAPTER 2

2 WORKPIECE & TOOL MODELLING

2.1 Geometric Model of Physical Simulation

The turning operation is the most common way of cutting cylindrical workpieces, accounting for approximately 25% of the metal's removal process. Turning tools of various shapes are used to cut various features such as cylinders with shoulders on both the left and right sides, slots, and end faces. The tools used to cut various workpiece materials have varying characteristics. The geometric features of an insert turning a workpiece are explored to forecast cutting force, cutting temperature, and tool life in the given parameter of turning. The insert is cutting a workpiece in Fig. 2.1(a), the insert is stationary, and the workpiece is rotating along the lathe axis. It clearly depicts how well the insert-sided cutting-edge contacts with the workpiece at a certain point in time. A spot on the side sharp end is sampled to illustrate the geometrical intricacy of this cutting. The tangent of the side cutting edge is obtained at this location, and the cutting speed direction is normal to the radius line of the point. Then, in Fig. 2.1, a plane normal to the tangent passes through the cutting and intersects with the insert and the workpiece, and the sectional view is depicted (b). The rake face is depicted in this illustration as the inserted upper surface towards the cutting edge. The rake angle is the angle formed by the rake face and the normal to the cutting speed.

Rake angles can be particularly dependent on the workpiece and insert materials. Inserts with negative rake angle angles are frequently used in roughing for more cutting power and higher cutting temperature. inserts with positive rake angles have been used in finishing to reduce cutting forces and improve surface roughness. The relief or flank face is the insert surface closest to the machined surface. The clearance angle is defined as the angle formed by a workpiece line and the flank. If the clearance angle is too narrow, the flank may rub against the machined surface, resulting in flank wear and poor machined surface quality. When the clearance is considerable, the cutting edge of the insert is weaker.

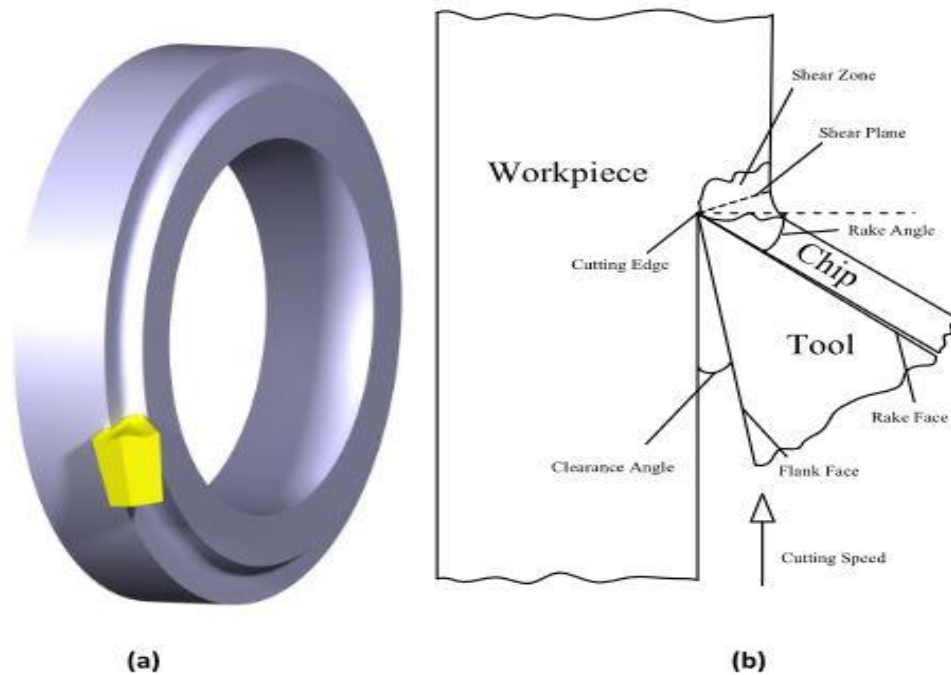


Figure 2.1 A 3-D geometric model of an insert cutting a workpiece in turning.

2.2 Modelling of the Workpiece

The workpiece is the initial product on which the machining is to be done for obtaining a final product that will be used for the purpose it was intended to. In every machining operation, the interactions between the cutting tool and the workpiece are crucial. The cutting process produces forces on both the tool and the workpiece as it passes through the workpiece. These forces have an impact on the process and, in some situations, can be damaging to the machine, tool, and final product. To avoid trashed components or tool or machine breakage, it is essential to understand these relationships beforehand machining a product.

The modeling of the workpiece is done with the help of Catia V5 software which is a Three-Dimensional Interactive Application. For modeling, the workpiece part design module of the software is used. First of all, a circle is made of a diameter of 25.5 mm on the y-z plane and then the sketcher is closed because our workpiece is a cylindrical workpiece. Now Pad command is used with the length of 150 mm to make the circle into a cylinder as our workpiece has a diameter of 25.5mm and a length of 150 mm. The Pad command will extrude the circle into the z-x plane direction. The 3D model created of the workpiece is shown in Fig. 2.2.

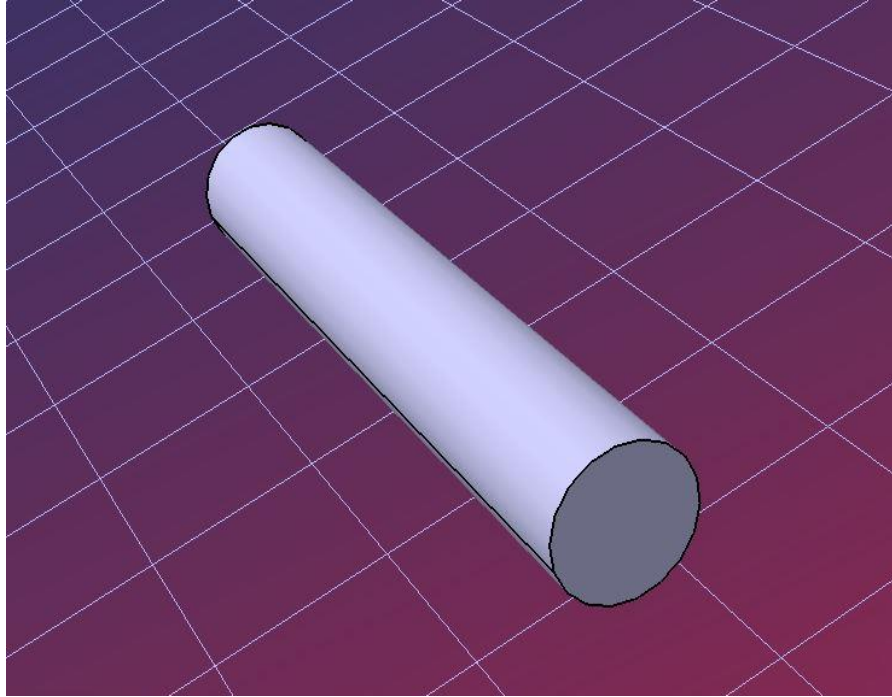


Figure 2.2 3D model of the Workpiece

2.3 Modelling of the Tool

A turning tool or the turning operation is comprised of a tool which is also called an insert and a tool holder. Typically, companies do not release 3D solid models of turning tools. To perform high operation simulation, the turning tool should be simulated with the very same geometry as the real tool shape. The specifications of the insert and tool holding characteristics should be acquired in accordance with ISO and corporate requirements for this purpose. Inserts are divided into three categories: roughing, semi-finishing, and finishing. They are also divided into two types: external and internal turning.

A turning process consists of a tool, sometimes known as an insert. Modeling of the tool is done in the Part Design option under the Mechanical design module of the software Catia V5. The tool will be made in the same file but in a different body than the workpiece, otherwise, the system will take the workpiece and tool as a single body and it will show errors in the geometry. First of all, a sketch is made of the tool's top view in the sketch on the x-y plane i.e., a triangle is made. After that, the sketcher is closed because the next command used is a 3D command. The next command used is a 3D command i.e., the pad is used to make the triangle into a 3D object. After that, all the angles and the slant heights are to be made by using the Pocket command. There is a hole to be made in between the model that will be used to hold the tool to the tool holder. A circle is made on the face where the hole is to be made. Then to make the hole, the pocket command is used and the hole is created. The 3D model created by the tool is shown in Fig. 2.3.

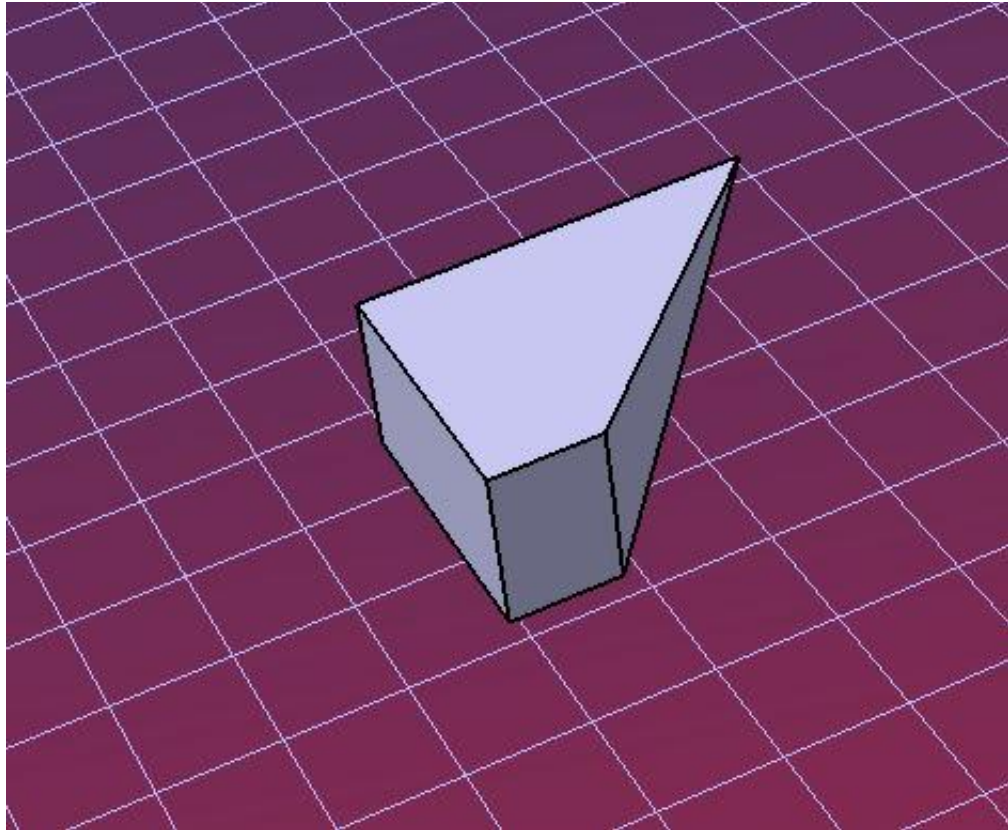


Figure 2.3 3D model of the Tool

2.4 Tool and Workpiece Used

An accurate model of the workpiece and the tool is made in the software Catia V5. Both the tool and the workpiece are made and compared with the real components used in the thesis. The tool–chip and tool-workpiece interfaces are those contact areas that directly participate in the cutting process. In this thesis, the cutting process used is Turning to reduce the diameter of a cylindrical aluminum alloy i.e., AA6082-T6 bar with a Carbide insert tool. The real Carbide insert tool and the cylindrical aluminum alloy i.e., AA6082-T6 are used for the specifications and the parameters of the 3D model created in the Catia V5 software. The real workpiece and the tool used are shown in Fig. 2.4 and Fig. 2.5 respectively.



Figure 2.4 A Cylindrical AA6082-T6 bar

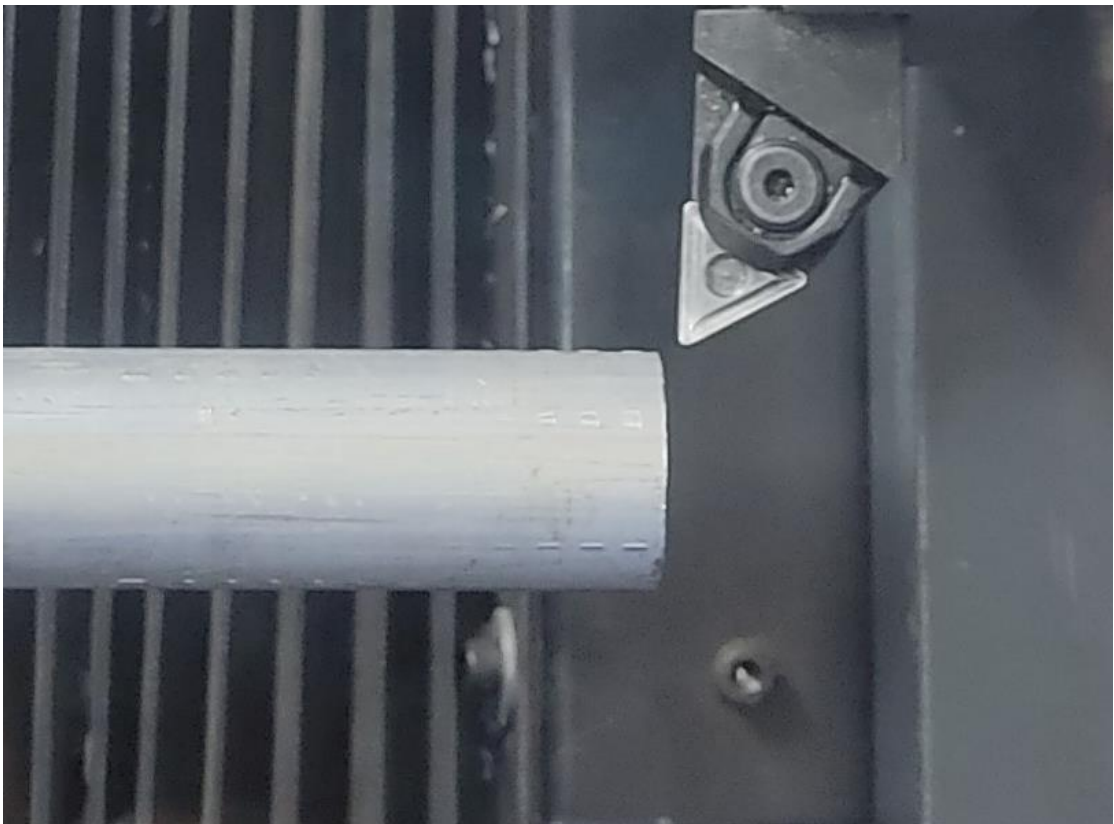


Figure 2.5 Carbide Insert Tool

2.5 Saving & Importing the Model for Analysis

The model created is to be saved in a way that the model should be able to be open in Ansys software. Catia V5 will save the file in the .catpart file extension which will not be able to open in Ansys R19.2. For the file to be able to be imported and used in Ansys R19.2 the file should be saved in the .stp or .iso file extension. After saving the file in Catia V5 with this extension we will exit Catia V5 and head to Ansys R19.2 software. A new file is opened for analysis in Ansys R19.2 software. In that new file choose the Explicit dynamics module of the software for the analysis in which we will perform our whole analysis. The screen we get after opening a new file for the Explicit dynamics module is shown in Fig. 2.6.

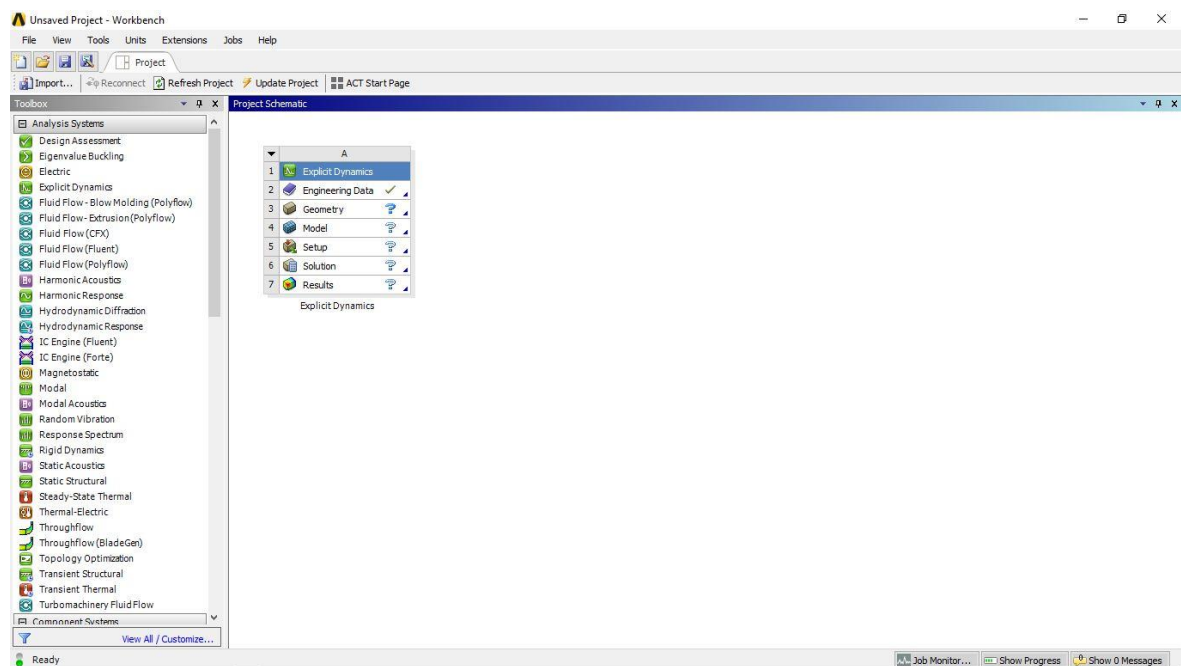


Figure 2.6 Explicit Dynamics Module Screen of Ansys R19.2 Workbench

The file can be named and the data is to be input for the analysis into the system. The Engineering Data is already ticked in the system but the settings and the data are the default data of the system. We will see about the data of the workpiece and the tool properties in the next chapter. Now we will import the geometry we made in Catia V5 into the geometry. Right-click on the geometry and choose the import geometry option from the different options available. Then we chose the file of the 3D model we made and saved it into the .stp extension and the geometry got imported into Ansys R19.2 software. The imported geometry is shown in Fig. 2.7.

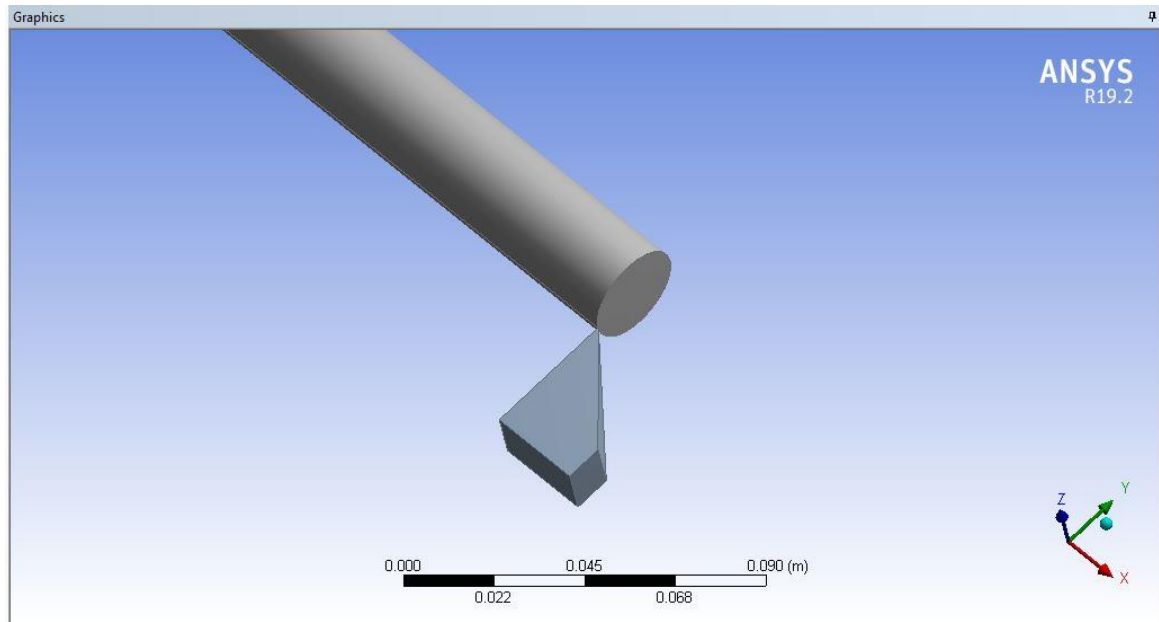


Figure 2.7 Imported Geometry to Ansys R19.2 software

The imported geometry is showing the workpiece, the tool, the tool holder, and the bot. There are two options to edit the imported geometry in Ansys R19.2, the Design Modeler and the Space Claim. Edit the imported geometry with Design Modeler and generate the model using add material command rather than using add frozen command. Add frozen command will freeze the model in its place and the analysis cannot be performed. So, we made sure Add material command is chosen, and then we generate the model. After that, the model is generated as shown in Fig 2.7.

CHAPTER 3

3 PROPERTIES OF MATERIALS USED

3.1 General Properties

A workpiece made of AA6082-T6 and a tungsten carbide-tipped tool were employed. Aluminum is among the most processed materials accessible today, hence AA6082-T6 was chosen as a workpiece. Aluminum follows steel in terms of consistency of implementation in machining operations due to its great machinability. Tungsten carbide is used as a tool because it keeps a sharper cutting edge than steel tools and enables quicker machining. The following characteristics must be present in a cutting tool: Hot Hardness, tenacity, Resistance to Wear, Chemical Inertness or Stability, Resistance to Shock, Lack of Friction, and Reasonable Price. In most cases, hardness is studied at room temperature. However, the phrase Hot hardness refers to durability at high temperatures. We know that when the temperature rises, the hardness reduces. Heat is created during the machining operation. At such a high raised temperature, the tool material has to be able to keep its hardness, wear resistance, and strength. The material must be robust enough to withstand the shock pressures that occur during continuous cutting operations without fracturing. It must be capable of withstanding vibrations caused by machining. The concept of wear refers to material loss. As the tool proceeds to cut, the cutting edge, which is continually in contact with the product, and the rake face (across whereby the chip passes) eventually lose material. As a result, the tool type must be worn-resistant in order to achieve an adequate tool life before the tool is indexed or removed.

The core material must be chemically stable or neutral to the job material to avoid any undesired interactions between both the tool material and the workpiece material. The cutting tool must be resistant to heat and physical shocks, especially in irregular cutting when the device connects and disconnects at periodic intervals. The material used for the tool should have a low coefficient of friction. As a result, the heat created is reduced, and tool life is extended. Tool material costs must be acceptable in a competing industrial setting to maximize profitability. Diamond tools, for example, are not commonly utilized because of their expensive price

Even if you're machining cast irons, low-alloy steels, or nickel-based alloys, all of these substances display 5 basic physical attributes in variable degrees. These qualities are abrasiveness, hardness, thermal conductivity, adhesion/ductility tendencies, and strain hardening. The ratios of distinct qualities in a particular workpiece greatly influence its

machinability. Slightly softer low-alloy steel has significant adhesion tendencies, which can cause edge accumulation on a cutting tool and diffusion wear. Poor heat conduction of a strong nickel-base alloy, on the other hand, might create severe cutting temperatures, causing a tool to distort and fracture. In principle, the stated alloying element mixture of a material specifies the type of cutting tools and cutting settings that will generate consistent and regular wear patterns and aid boost production. However, the fact is that cutting tools and settings specified for a certain workpiece may not achieve the anticipated results, and this is frequently due to variation in material composition. Seco collaborated with steel suppliers and other metalworking-related organizations to build an analytical system that evaluates workpiece parameters to better understand how the five variables impact machinability. Data from quantitative measurements of the five material attributes are shown in Fig. 3.1 on a five-pointed grid or pentagram, with smaller returns in the center and high values towards the edges. The region encircled by the data points is a graphical representation of the substance's trends. Machinists may best match tool characteristics and cutting settings to the real attributes of the workpiece by using the pentagram.

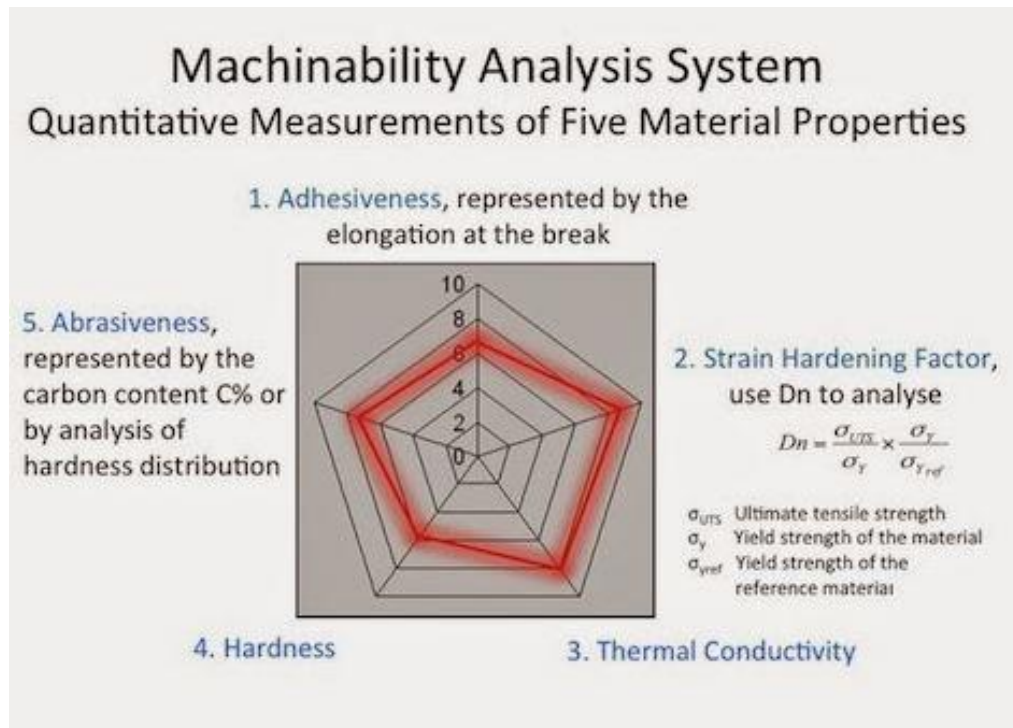


Figure 3.1 Quantitative Measurements of Five Material Properties

3.2 Properties of the Workpiece Used

The Workpiece Chosen for this thesis is an alloy of aluminum, as aluminum is the second material used in place of steel which is also efficient and also good in terms of frequency of execution. The Aluminum alloy used in this thesis is AA6082-T6. Aluminum alloy 6082 is a moderate alloy with excellent adhesion. It is also the most powerful of the 6,000 different

alloys. Alloy 6082 is also designated as a structural alloy. 6082 is perhaps the most commonly utilized alloy for machining in plate form. Although 6082 is a comparatively recent alloy, its increased strength has seen it supplant 6061 in numerous applications. A considerable quantity of manganese is added to regulate the grain structure, resulting in a stronger alloy. Alloy 6082 is difficult to make thin-walled, complex extrusion forms. The projected surface texture is not as fine as that of other 6000 series alloys of comparable quality. The properties of the workpiece are to be fed to the system in the Engineering data module of the Ansys R19.2 software. The data entered in the Engineering data module of Ansys R19.2 software is shown in Figure 3.2.

	A	B	C	D	E
1	Property	Value	Unit		
2	Material Field Variables	Table			
3	Density	2.71	g cm ⁻³		
4	Specific Heat, C _p	900	J kg ⁻¹ C ⁻¹		
5	Shear Modulus	2.69E+10	Pa		
6	Shock EOS Linear				
7	Gruneisen Coefficient	2.1			
8	Parameter C1	5380	m s ⁻¹		
9	Parameter S1	1.337			
10	Parameter Quadratic S2	0	s m ⁻¹		
11	Johnson Cook Failure				
12	Damage Constant D1	0.0164			
13	Damage Constant D2	2.245			
14	Damage Constant D3	-2.798			
15	Damage Constant D4	0.007			
16	Damage Constant D5	3.65			
17	Melting Temperature	555	C		
18	Reference Strain Rate (/sec)	1			

Figure 3.2 Properties view in Engineering Data module of Ansys R19.2

3.2.1 Chemical Composition of the Workpiece

It is one of the most widely used alloys in its class. It is normally manufactured by extrusion and rolling, but it is not utilized in casting as a wrought alloy. It may also be forged and clad, however, this is not typical with this alloy. It cannot be work hardened, although it is frequently heat-treated to generate tempers with greater strength but less ductility. This aluminum alloy AA 6082-T6 is a composition of different chemical mixtures and substances like aluminum, silicon, iron, etc. All the mixtures present in the alloy are in some composition percentage. The most percentage substance is aluminum and that is why it is called an aluminum alloy. The chemical composition that is present in the alloy is given in table 3.1. The composition is presented based on the weight percentage available in the aluminum alloy.

Table 3.1 Chemical Composition(wt.%) of AA6082-T6

Al	Si	Fe	Cu	Mn	Mg	Cr	Zn	Ti	Others
95.2-98.3	0.7-1.3	0.5	0.1	0.4-0.1	0.6-0.1	0.25	0.2	0.1	0.15

3.2.2 Mechanical Properties of the Workpiece

This document's material is a cylindrical AA6082-T6 bar with a length of 150mm. AA6082-T6 is an aluminum alloy with strong corrosion resistance that is primarily used for machining. It has more strength than other alloys and, as a result, is replacing other aluminum alloys in the industry. The mechanical properties used for this thesis are density, Specific Heat, Shear Modulus, etc. These properties are then tested and verified properties of Al 6082-T6 and are used here for the analysis in the Ansys Software. The standard units used in this thesis for mechanical properties are SI units. The mechanical properties of the workpiece are given in table 3.2 with the units which are used.

Table 3.2 Mechanical Properties of the Workpiece

Property	Value (Unit)
Density	2710 (kg/m ³)
Specific Heat	0.9 (J/gK)
Shear Modulus	2.69e ¹⁰ (Pa)
Melting Temperature	555(°C)
Reference Strain Rate	1 (/s)

3.2.3 Failure Model of the Workpiece

The Johnson-Cook failure model is utilized for the failure concept, with a linear connection between the shock velocity and the particle velocity. Because of its simplicity of construction, ease of validation, and several material characteristics offered by Johnson and Holmquist [1989], the Johnson-Cook fracture model is extensively used. Johnson and Cook [1985], on the other hand, only calculated the positive range of stress triaxiality based on certain tensile and shear tests, and no tiny or minus values of stress triaxiality are stated. Perhaps one function is incapable of expressing two distinct fracture processes when stress triaxiality changes from negative to favorable: shear decohesion and void development. It is demonstrated that aluminum ductility is not a monotonic function of stress. Researchers

expanded the Johnson-Cook fracture model in various ways to properly use it. Liu et al. [2014] demonstrated that the Johnson-Cook fracture model may be applied in machining operations simulation as a fracture point paired with damage development.

An additional failure property is given to the model and it is the Shock EOS in a linear manner in which two parameters and a Gruneisen coefficient are used. The Gruneisen parameter, established after Eduard Gruneisen, defines the influence of altering the volume of a crystalline structure on its vibrational characteristics, as well as the impact of temperature changes on the size or dynamics of the crystalline structure.

Table 3.3 Failure Properties of the Workpiece

Johnson Cook Failure	
D1	0.0164
D2	2.245
D3	-2.798
D4	0.007
D5	3.65
Shock EOS (Linear)	
Gruneisen Coefficient	2.1
Parameter C1	5380 (m/s)
Parameter S1	1.337

3.3 Properties of the Tool Used

Cemented carbide is a tough substance that is widely utilized in cutting tool materials and other engineering products. It is made up of tiny carbide particles that are glued together in a compound by a binder metal. The aggregate in cemented carbides is often tungsten carbide (WC), titanium carbide (TiC), or tantalum carbide (TaC). In industrial applications, the terms "carbide" or "tungsten carbide" commonly apply to these cemented compounds. Carbide cutters, like most cases, leave a superior surface quality on the item and allows for quicker machining over high-speed steel or other alloy steel. Carbide tools are more resistant to heat at the cutter-workpiece contact than ordinary high-strength steel tools. Carbide is typically ideal for cutting difficult materials like carbon steel or stainless steel, as well as in instances in which other cutting tools would wear out faster, such as high-volume manufacturing runs. The properties of the tool are to be fed to the system in the Engineering data module of the Ansys R19.2 software. The data entered in the Engineering data module of Ansys R19.2 software is shown in Figure 3.3.

	A	B	C	D	E
1	Property	Value	Unit		
2	Material Field Variables	Table			
3	Density	20	kg m ⁻³		
4	Isotropic Elasticity				
5	Derive from	Young's Modulus and Poisson...			
6	Young's Modulus	6E+11	Pa		
7	Poisson's Ratio	0.2			
8	Bulk Modulus	3.333E+11	Pa		
9	Shear Modulus	2.5E+11	Pa		
10	Specific Heat, C _p	0.000184	J kg ⁻¹ K ⁻¹		

Figure 3.3 Properties view in Engineering Data module of Ansys R19.2

Cemented carbides are matrix alloy composites composed of carbides as the aggregates and a metallic adhesive as the matrix. The architecture of a carbide cutter is thus theoretically identical to that of a grinding wheel, with the exception that the abrasives are much small; macroscopically, the material of a carbide cutter seems homogenous. It binds tungsten and carbon to produce an exceptionally compact crystal structure known as hexagonal crystal, with Young's modulus nearly twice that of steel. Table 3.4 lists the mechanical qualities of the tool. Some of the characteristics in the table are obtained from other values, such as shear modulus and bulk modulus, which are derived from young's modulus and poison's ratio, respectively.

Table 3.4 Mechanical Properties of the Tool

Property	Value (Unit)
Density	20 (kg/m ³)
Young's Modulus	6e ¹¹ (Pa)
Poisson's Ratio	0.2
Bulk Modulus	3.33e ¹¹ (Pa)
Shear Modulus	2.5e ¹¹ (Pa)
Specific Heat	1.84e ⁻⁷ (J/gK)

CHAPTER 4

4 CONNECTIONS AND MESHING

4.1 Coordinate System

A coordinate system in geometries is a system that involves one or more integers, or parameters, to define the point's position or other components of the geometry on a manifold, which is also known as Euclidean space. The ordering of the parameters matters, and they are sometimes identified by their position in an ordered tuple, and sometimes by a letter, as in "the x-coordinate." In mathematical concepts, the parameters are assumed to be actual figures, but they can also be complex numbers or members of a more abstract representation, such as a commutative ring. The use of a coordinate system allows geometry issues to be transformed into numerical problems and vice versa and this is the foundation of computational geometry.

In this Thesis there are two different types of coordinate systems employed, one is a global coordinate system used for the whole system and the other one is a cylindrical coordinate system used for the workpiece. The detailed study of the coordinate system used in this thesis is done below in sections 4.1.1 and 4.1.2 respectively.

4.1.1 Global Coordinate System

A Global Coordinate System is a coordinate system that is used to locate the whole system or a single body in the system. They are used to specify the spatial coordinates of nodes and key points. They may be used to detect and identify physical model and simulation model items depending on their spatial locations. The global coordinate system determines a component's location and translation in space. Local coordinate systems specify how branches and body parts interact with respect to joints. Global Coordinate system is used in this thesis to locate the whole system in the coordinate, especially the tool as workpiece has its own coordinate system, in which it rotates. The tool propagates towards the workpiece in the system based on the global coordinate system. The global Coordinate system is defined by the X, Y, and Z-axis as shown in Fig. 4.1.

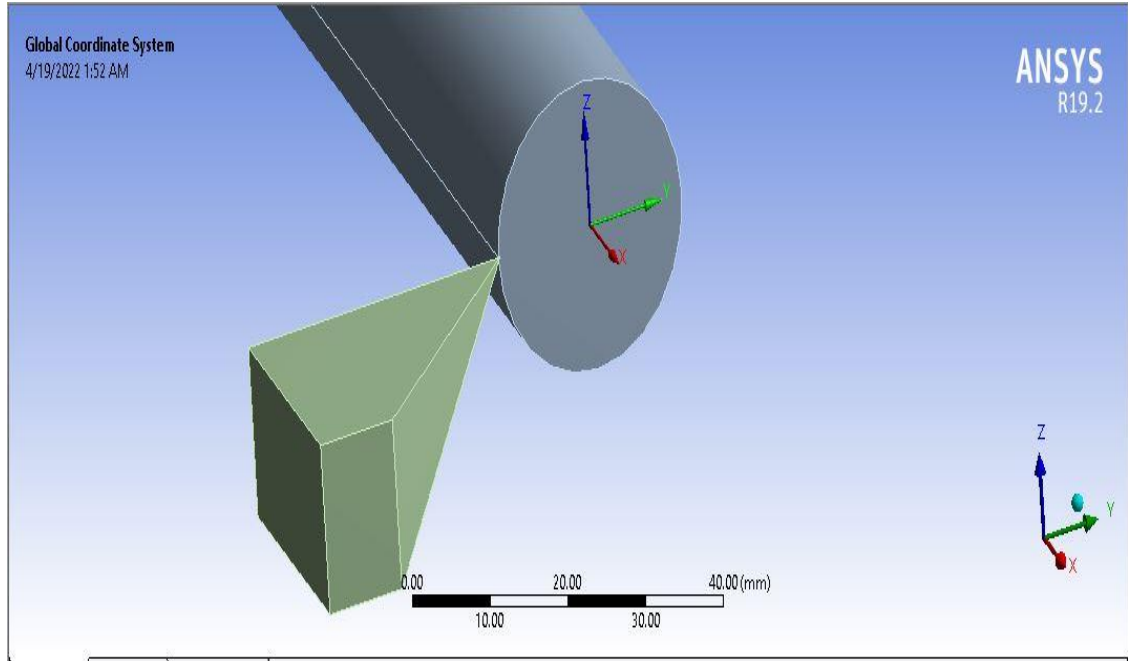


Figure 4.1 Global Coordinate System

The red-colored axis shown in the above Fig. 4.1 is the x-axis, green is depicting the y axis and the blue color is depicting the z-axis of the global coordinate system. The point where all three axes are intersecting is called the origin point of the system.

4.1.2 Cylindrical Coordinate System

A Cylindrical Coordinate System is a coordinate system that is used to locate the cylindrical body in the system. They are used to specify the spatial coordinates of nodes and key points of a cylindrical body available in the system. They may be used to detect and identify physical model and simulation model items depending on their spatial locations. The cylindrical coordinate system determines a cylindrical component's location and translation in space. In a cylindrical coordinate system, the R, Y, and Z axes are represented by X, Y, and Z. Non-zero Y deformations are understood as translational displaced quantities, $Y = R$ when employing a cylindrical coordinate system. Because they are represented as straight deformations, it is only an acceptable estimate for small levels of rotational movement. Figure 4.2 shows a cylindrical coordinate system established by the X, Y, and Z axes used in this thesis and the analysis system.

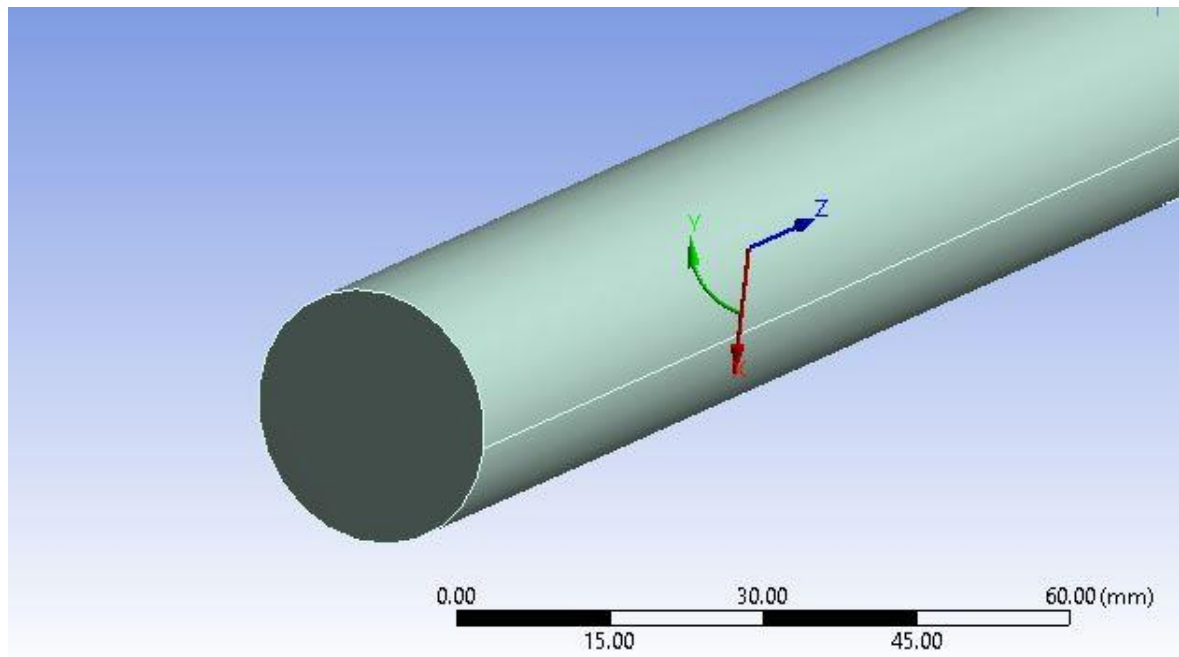


Figure 4.2 Cylindrical Coordinate System

The red-colored axis shown in the above Fig. is the x-axis, green is depicting the y axis and the blue color is depicting the z-axis of the cylindrical coordinate system. The point where all three axes are intersecting is called the origin point of the cylindrical body. It is hard to understand the position of the axis shown in Fig. 4.2 because two coordinate systems are acting on the same body, the one in the global coordinate system acting on all bodies i.e., the whole system, and the other one is the cylindrical coordinate acting on the single cylindrical workpiece body. For a better understanding of the cylindrical coordinate system, the axis should be placed properly. Fig. 4.3 gives a better understanding of the cylindrical coordinate system.

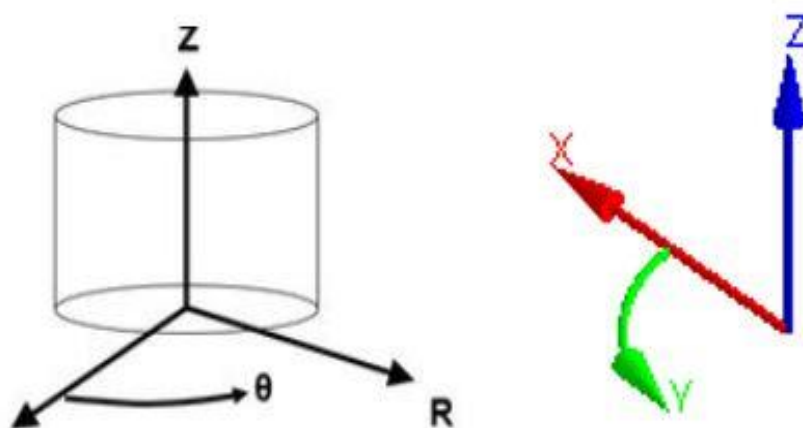


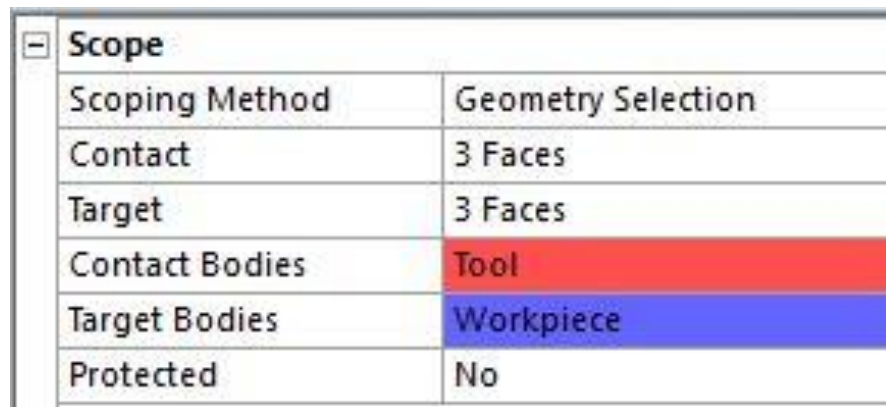
Figure 4.3 Cylindrical coordinate system with respect to angle

4.2 Connections

Ansys R19.2 Explicit Dynamics module offers a variety of connection options like Connected by contact, Connected by joint, and Connections for beams. In this thesis, the type of connection used is connected by contact as the tool and workpiece are contacting each other and after this connection, the cutting action occurs. Every connection provides unique choices for accurately representing the passage of forces/moments between bolts and assemblies. The depiction of the bolt influences the decision of connection type, and likewise. The contacts used in the thesis are further explained in the next section.

4.2.1 Contacts

The contacts are given to the system by selecting the faces of the tool and the workpiece as the contact body and as the target body. Contact issues are extremely complex and need a substantial amount of computational ability to solve. It is vital to comprehend the physics of the problem and spend the effort necessary to configure your model to operate as efficiently as possible. You must detect potential points of contact during the deformation of your model. Once prospective contact surfaces have been discovered, they are defined using target and contact elements, which then follow the kinematics of the deformation process. A contact pair's target and contact components are linked together via common real support data. The type of contact used in the thesis is the Frictional contact between the tool and the workpiece. Scope option of the setting of contact shows the faces of everybody that is selected for the contact of the tool and the workpiece. The scope option is shown in Fig. 4.4.



Scope	
Scoping Method	Geometry Selection
Contact	3 Faces
Target	3 Faces
Contact Bodies	Tool
Target Bodies	Workpiece
Protected	No

Figure 4.4 Scoping Method of Contact

In Fig. 4.4 it is shown that the contact body is the tool and the faces selected for the contact body are 4 faces. The additional critical capability is the ability to modify the attributes of the contact pairs as needed. As previously explained, the attributes comprise actual constant values and key option values. The Contact Properties button in the contact

manager provides a simple interface for reviewing and modifying the attributes of the chosen contact pairs also. The contact zone can be random; however, for the most economical solution (mainly in terms of CPU time), you may wish to design smaller, localized contacting areas; nonetheless, make sure your areas are sufficient to record every essential interaction. Even though the element real constant values do not vary, distinct contact pairings should be specified by a separate real constant set. There is no limit to the number of surfaces that can be used. The contact body i.e., the tool with the selected faces is shown in Fig. 4.5.

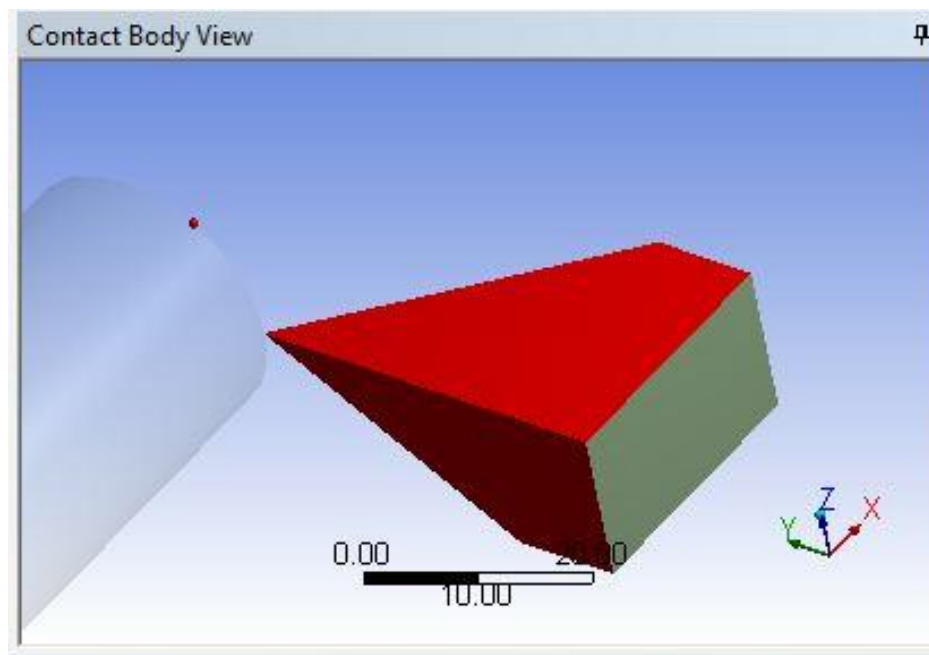


Figure 4.5 Contact Body

In Fig. 4.4 it is also shown that the target body is the workpiece as the workpiece is cutting in the analysis and the faces selected for the contact body are 3 faces that are coming in contact with the tool in the initial state when the turning process starts. Contact elements are prevented from entering the target surface. Target elements, on the other hand, can pass through the contact surface. The designation for rigid-to-flexible contact is self-evident: the target surface is always the rigid surface, and the contact surface is always the deformable surface. The decision of whether the surface is labeled contact or target for flexible-to-flexible contact might result in a varying degree of penetration and hence influence solution accuracy. On the very same target surface, you cannot mix rigid and deformable target elements. Ansys assigns a deformable state to target elements that have underneath components and a rigid status to target components that do not have underneath components during the solution. An issue in the solution will arise if a section of the underlying components of a deformable surface is eliminated. The target body i.e., the workpiece with the selected faces is shown in Fig. 4.6.

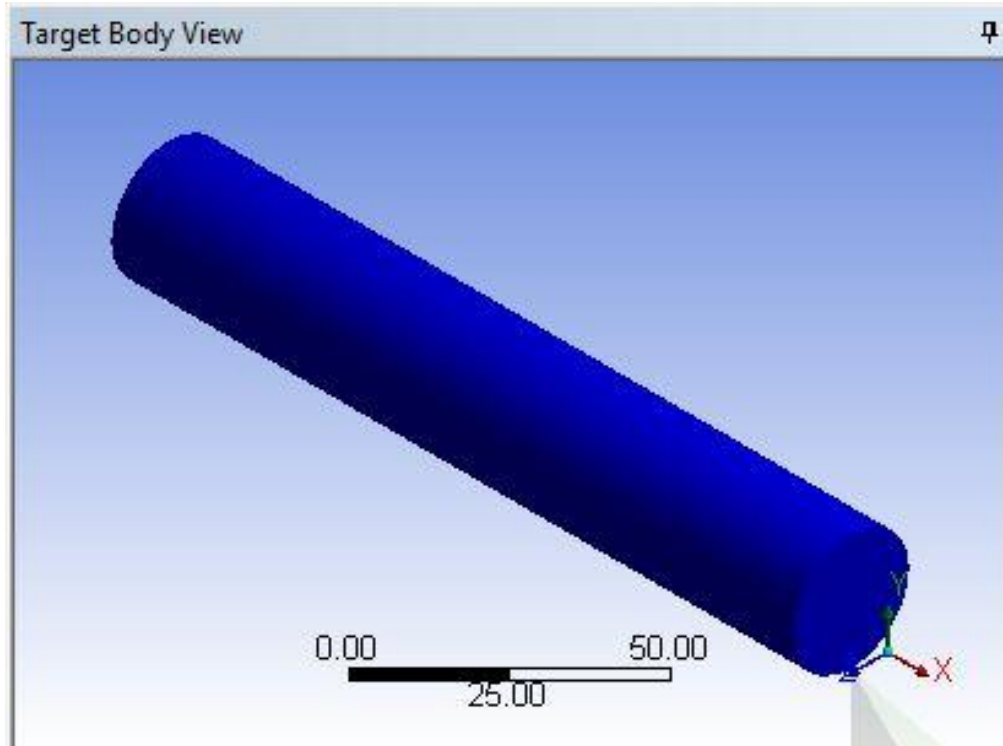


Figure 4.6 Target Body

4.2.2 Body Interaction

Underneath connections, the body interaction box is used to define global connection parameters for explicit dynamics. At the beginning of the trials, nodes that penetrate some other component will be disregarded for contact and should be avoided. Each body interaction object initiates a body interaction for the entities that are scoped in the system. There are four types of body interactions bonded, no separation, frictionless, rough, and frictional.

The type of body interaction used in this thesis is frictional with a friction constant value of 0.4 and a dynamic constant value of 0.1. The decay constant is not used for this analysis and left default as zero because no decaying is happening in the system as the analysis is running for a very small-time step. All encounters that occur at the very same moment are recognized first. The program's reaction is then computed to save energy and momentum. Forces are computed throughout this procedure to guarantee that the final location of nodes and faces doesn't result in additional infiltration at that point time. In a particular cycle, the decomposition response algorithm is more impulsive than the punishment technique. In some cases, this might result in enormous hourglass energies and energy mistakes. The body interaction folder from the Ansys explicit dynamics module is shown in Fig. 4.7.

Details of "Body Interaction"	
[-] Scope	
Scoping Method	Geometry Selection
Geometry	All Bodies
[-] Definition	
Type	Frictional
Friction Coefficient	0.4
Dynamic Coefficient	0.1
Decay Constant	0.
Suppressed	No

Figure 4.7 Body Interaction

4.3 Meshing

Mesh generation, also known as two-dimensional and three-dimensional grid generation, is the process of splitting complicated shapes into pieces that may be used to discretize an area. Meshing is the act of breaking down an item's continuous geometrical area into thousands or more forms to adequately define the physical shape of the subject. This procedure often takes up a large amount of the time spent obtaining simulated results. When it comes to numerical simulations, meshing plays a vital role. Among the most important elements to consider when ensuring simulation accuracy is the creation of a high-quality model. The cornerstone of engineering simulation is the creation of the most suitable mesh because the mesh determines the simulation's accuracy, resolution, and performance. Machines cannot perform simulations on the real geometric shape of the CAD system because the system of equations cannot be implemented to irregular shapes.

All 3-dimensional meshing techniques need geometry to be made up of solid entities. If an imported geometry comprises surface entities, further procedures must be taken to transform it into a 3-dimensional solid before generating a three-dimensional model in the ANSYS Meshing Application. Although surface bodies can also mesh with the surface meshing algorithms available for surface meshing. Surface meshing is not employed in this thesis as there is no need for surface meshing on solid bodies. The meshing of the workpiece and the tool is shown in Fig. 4.8 and Fig. 4.9 respectively.

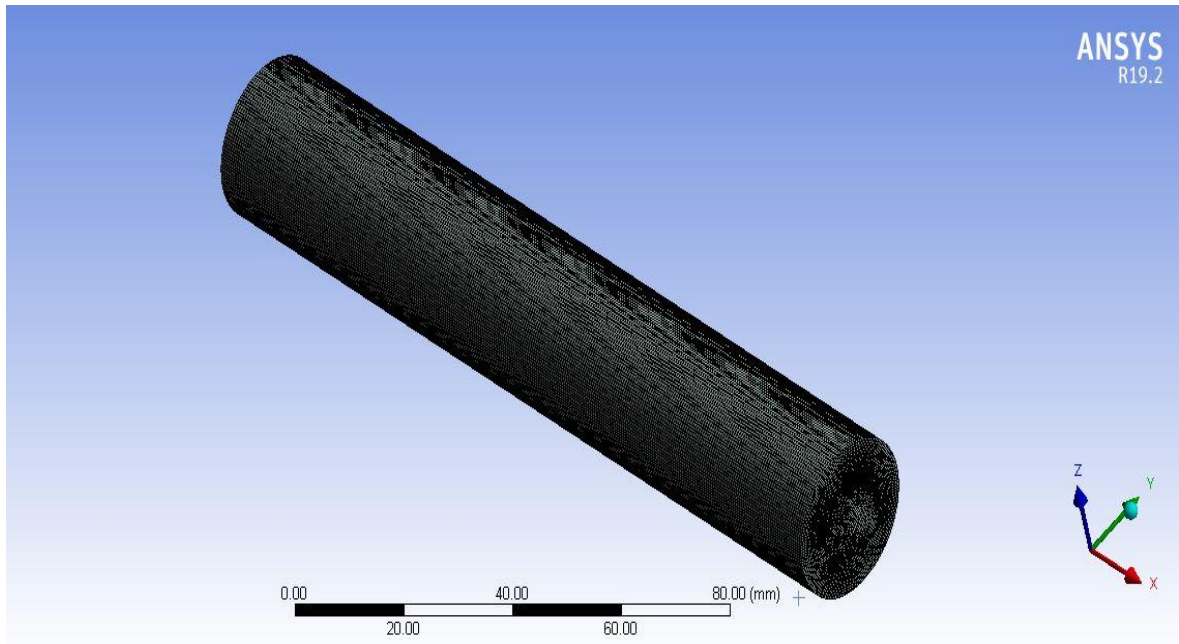


Figure 4.8 Meshing of the Workpiece

The size of the mesh used is 0.5 for the meshing of the workpiece because the workpiece is deforming in the turning process. The cutting operation is taking place on the workpiece so the workpiece meshing should be fine and small related to the tool. The meshing size of the tool is taken as the default value of the Ansys explicit module. This is the reason that the meshing of the tool and tool holder is more visible than the workpiece.

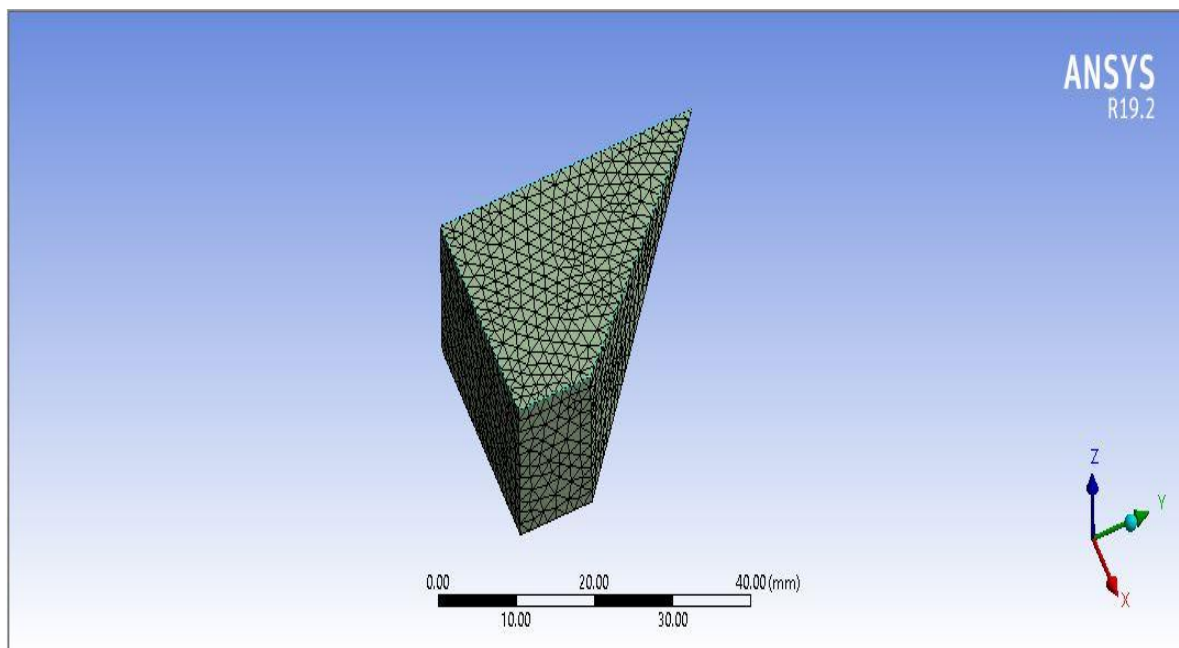


Figure 4.9 Meshing of the Tool & the Tool Holder

4.3.1 Size of Mesh

Mesh size affects both numerical precision and computing time. Sizing options give us more control over some properties which are mesh expansion from tiny to big sizes depending on a preset rate of growth, Sophistication based on curves and angles among normal neighboring mesh elements, and the number of mesh pieces used to bridge the gap among different geometric entities. Element Size, Growth Rate, Max Size, and Curvature Min Size / Proximity Min Size are all sizing controls. Curvature Min Size/Proximity Min Size and Max Size requirements describe the global upper and lower limits permitted element size, accordingly. The Element Size specification specifies the global maximum permissible length of the elements generated by the available techniques. When the Physics Preference is set to Explicit dynamics, Adaptive Resolution is set to Program Controlled means the default value is 4. The default value for all other Physics Preferences is 2. Mesh size is one of the most typical FEA issues.

There is a delicate difficulty in mesh sizing that a larger item provides a poor result, while smaller elements cause the computation to take so long that the results are not obtained at all. You never truly know what exactly your element size is on this scale. The Growth Rate reflects an increase in element edge length with each level of elements added to the edge or face. A growth rate of 1.2, for example, leads to a 20% increase in element edge length with each subsequent level of elements. Adaptive Sizing is used with the mesh defeaturing property of the mesh sizing. The span angle center should be fine for the mesh to be fine and for the solution to be more accurate. After mesh sizing is done, we get three values and those are Bounding Box diagonal, Average Surface area, and Minimum Edge length. The mesh sizing used in the thesis is shown in Fig. 4.10.

Sizing	
Use Adaptive Sizing	Yes
Resolution	Default (4)
Mesh Defeaturing	Yes
<input type="checkbox"/> Defeature Size	Default
Transition	Slow
Span Angle Center	Fine
Initial Size Seed	Assembly
Bounding Box Diagonal	187.17 mm
Average Surface Area	1390.6 mm ²
Minimum Edge Length	10.0 mm

Figure 4.10 Mesh Sizing

4.3.2 Quality of the Mesh

Mesh Quality is the property of the mesh which allows a numerical Partial Differential Equation simulation to be done with faithfulness to the physical mechanisms, precision, and efficiency. Mesh-based applications require precision and efficiency. Many factors influence accuracy and efficiency, including the governing equations, the solution, the method of discretization, linear solvers and preconditions, and mesh quality. Interpolation Error Bounds are used to address accuracy. The traditional emphasis in FEM is on the asymptotic behavior of the limits, but they may also be studied in terms of mesh quality.

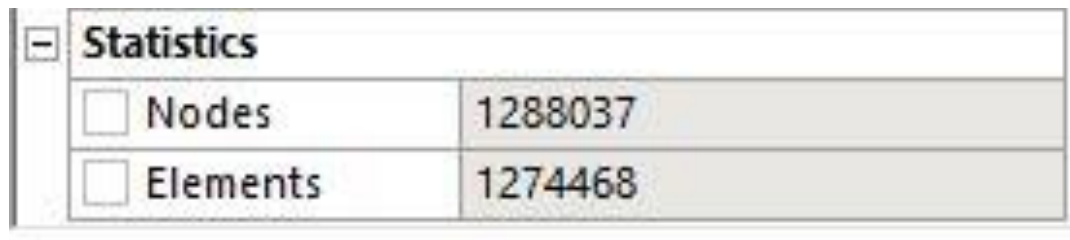
The mesh attributes that occur in the warning statements frequently need not correlate to every typical mesh quality measurement. Mesh Quality too is important in the development of basic meshes that will be customized to the answer further on. Parametric mesh quality may be measured using a variety of measurements, metrics, and functions. In industry, it is widely utilized. The integrity of a global mesh may be assessed using norms or p-means of local quality indicators. When it comes to computational models, the outcomes are only as great as the mesh - that is, a "bad" mesh would provide "bad" or erroneous results. That's why it is very important to check that the mesh is of good quality or good enough to produce accurate and trustworthy results. We can use skewness to measure mesh quality, but the ideal way is to check the resultant error and assess if the amount is appropriate for the given situation and required precision. The majority of ANSYS mistake estimations are produced by analyzing alternative techniques of result dispersion within the components. For the mesh metric of the system aspect ratio of the mesh is used. The quality of the mesh in numerical results is shown in Fig. 4.11.

[-] Quality	
Check Mesh Qua...	Yes, Errors
<input type="checkbox"/> Target Quality	Default (0.050000)
Smoothing	High
Mesh Metric	Aspect Ratio
<input type="checkbox"/> Min	1.0366
<input type="checkbox"/> Max	9.9832
<input type="checkbox"/> Average	1.6589
<input type="checkbox"/> Standard Devi...	0.47771

Figure 4.11 Quality of the Mesh

4.3.3 Statistics of Mesh

Rather than only conducting a visual check, the quality of a mesh may be judged most efficiently by focusing on various statistics, such as maximum skewness. Unstructured grids, in contrast to structured grids, are virtually difficult to comprehend with merely a graphical layout. Ansys may provide the lowest, maximum, and average values of cell size, skewness, aspect ratio, or change in size, warp, squish, edge ratio, and the overall number of every data element. Statistics of the mesh show the quality of the mesh with respect to the number of nodes and elements. In this mesh, we have the number of nodes as 1227869 and the number of elements as 1271803. The statistics table of the Ansys explicit dynamic module is shown in Fig. 4.12.

The image shows a software window titled "Statistics" with a minus sign icon in the top-left corner. It contains a table with two rows. The first row has a checkbox, the text "Nodes", and the value "1288037". The second row has a checkbox, the text "Elements", and the value "1274468".

Statistics	
<input type="checkbox"/> Nodes	1288037
<input type="checkbox"/> Elements	1274468

Figure 4.12 Statistics of the Mesh

CHAPTER 5

5 BOUNDARY CONDITIONS & ANALYSIS SETTINGS

5.1 Boundary Conditions

A boundary condition tells us about a mathematical function's behavior on the border or the boundary up to its defined region. Boundary conditions are limitations that must be met to solve a finite volume issue. A boundary value problem is a differential equation PDE (or system of a partial differential equation) that must be resolved in a domain with a specific set of parameters on its border. It differs from the "starting problem based," in which only one end of the interval's criteria is known. Boundary value issues are particularly significant because they simulate a wide range of processes and functions, including solid mechanics, heat transport, fluid mechanics, and acoustic diffusion. They naturally emerge in any issue based on a differential equation that must be resolved in space, whereas initial value problems are often problems that must be addressed in time. Jacques Charles François Sturm (1803-1855) and Joseph Liouville (1809-1882) explored the eigenvalues and the eigenvectors of a 2nd order differential equation for only linear problems and researched boundary condition issues extensively. They investigated the requirements that ensure the existence and uniqueness of the differential problem solution, as well as how boundary conditions impact it. The Sturm-Liouville theory is critical for every computing issue since it helps us to learn if an issue is "well-posed" as well as how to acquire a solution. Boundary condition difficulties exist in many disciplines of physics, as they do in any physical differential equation. Problems involving the wave function, such as determining normal waves, are sometimes referred to as boundary condition problems. The Sturm-Liouville issues are a wide family of critical boundary condition problems. The eigen functions of a differential operator are used to analyze these situations. To be resolved, both ordinary differential equations and partial differential equations require boundary conditions. A wide variety of border constraints could be applied to the domain's boundary. The selection of the boundary condition is critical for the settlement of the mathematical problem: a poor imposition of the boundary condition may result in solution divergence or convergence to an incorrect result.

Boundary conditions are both realistically necessary for identifying the issue and are of major relevance in computational fluid dynamics. This is because the application of numerical techniques and the resulting quality of calculations are highly dependent on how they are quantitatively addressed. Nowadays, the requirement for computational analysis of systems with shifting boundaries has grown and become even more complex. From such

foundations, particle process simulation, one of which is high flexibility in modeling boundaries involving violent motion, has gained increasing attention as a new potential computing platform in a variety of sectors of science and technology. Moving boundary issues include flow caused by moving bodies, constant flow, flow including air pockets, flow following phase transformation, and fluid-structure contact. When working with such moving or deformed borders, classic mesh techniques such as the finite difference method, finite element method, and finite volume approach often have difficulty computing the geometric shape of the boundary appropriately. Boundary conditions, which take the shape of differential algorithms, impose a set of extra restrictions on the issue along defined borders. Boundary conditions are used in both ordinary differential equations and partial differential equations. There are five types of boundary conditions and those are Dirichlet, Neumann, Robin, Mixed, and Cauchy. Out of these five boundary conditions, two are the most common and those are Dirichlet and Neumann. We will address in this thesis only the linear boundary conditions for the issues of explicit dynamics used for the analysis, which indicate a linear relationship between the function and its partial derivatives. We cannot usually describe the gradients at the border since it is too restricted to enable results. We may and frequently must indicate the component normal to the boundary in physical situations.

5.1.1 Initial Conditions

Ordinary differential equation results are rarely distinct (integration constants appear in many places). Of course, this is also an issue partial differential equation. Governing partial differential equations are often described by a set of the border or initial conditions. An initial condition is similar to a boundary condition, except it is applied in the time direction. Not that all boundary conditions have results, but science typically dictates what makes perfect sense. The essential distinction between both the arbitrary nature of integrating constants in Ordinary differential equations and Partial Differential Equations is that they are constants, Partial Differential Equations solutions contain arbitrary functions. For the initial condition in explicit analysis, a pre-stress initial condition is taken sometimes but for the analysis in this thesis, no initial condition is taken as there is no pre-stress in acting on the tool or the workpiece.

5.1.2 Displacement to the Workpiece

The workpiece will be rotating in its axis for the cutting process to be performed on it. A displacement is given to the workpiece to rotate the workpiece at its axis as it would be rotating with the chuck in the real process on the same axis. For this rotation of the workpiece, we made a cylindrical coordinate system. So, this cylindrical coordinate system will be selected for the rotation of the workpiece. For the displacement to work on the workpiece it is important to select the faces one by one instead of selecting the whole body at a time. There are three faces selected for the displacement setting to work on the

workpiece. The end time used for the analysis is 0.0001 s as the process will take a very small time to finish. If we take a large end time, we will miss the calculated solution in between the time step. The rotation of the workpiece is employed on the y-axis of the cylindrical coordinate system. At the end time, the degree of rotation chosen for the analysis is 100°. A representation of the boundary condition i.e., displacement employed on the workpiece is shown in Fig. 5.1.

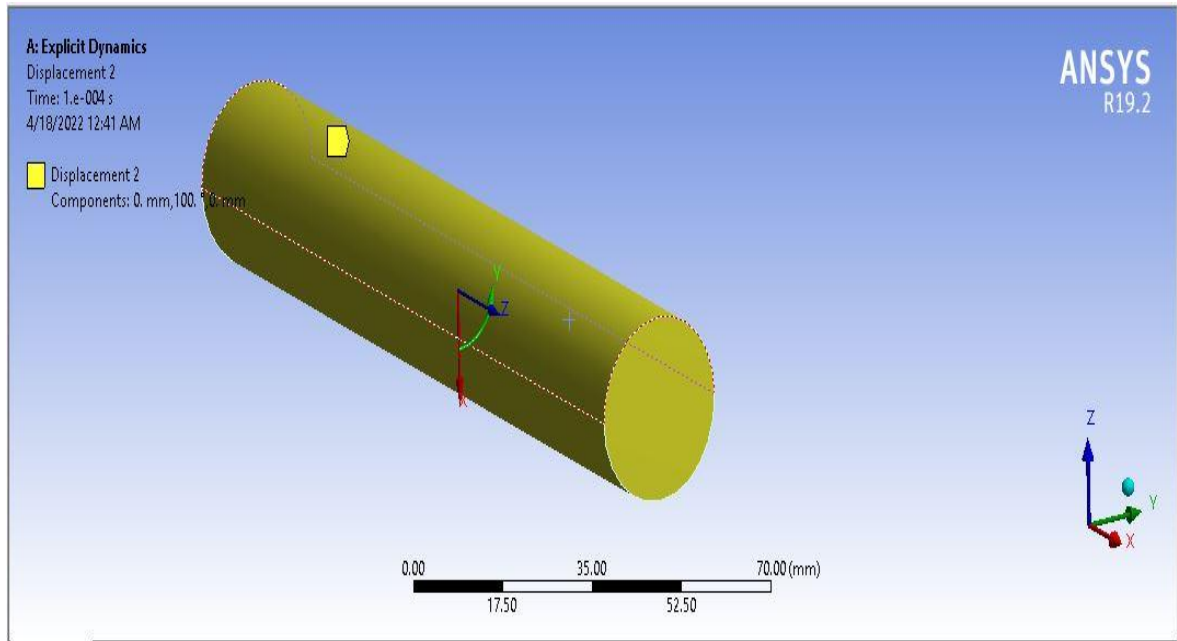


Figure 5.1 Displacement employed on Workpiece

There are two options available to select the details of the displacement i.e., scope and definition. Scope provides details about the selection of the geometry and the faces chosen for the displacement employed in the turning process. The definition provides the details and the options available for the employment of the displacement to a body and in this case the workpiece. The type of displacement is defined by the components of the axes. The coordinate used for the workpiece is a cylindrical coordinate system. The details of the displacement employed on the workpiece are shown in Fig. 5.2.

The only data remaining about the displacement is the details about the axes where the displacement is taking place. This data is shown in two places, one is in the details with the components and the second one is in the tabular form. In the tabular form, the displacement on the y-axis is shown concerning the time step taken or the end time taken. The table also shows all the data, if multiple displacement point is used in the system. For this thesis, there

is only one displacement point is used. The coordinate system shows the data of the axes available to the system in a tabular form which is shown in Fig. 5.3.

Details of "Displacement 2"	
Scope	
Scoping Method	Geometry Selection
Geometry	3 Faces
Definition	
Type	Displacement
Define By	Components
Coordinate System	Cylindrical Coordinate System
<input type="checkbox"/> X Component	0. mm (step applied)
<input type="checkbox"/> Y Component	100. ° (ramped)
<input type="checkbox"/> Z Component	0. mm (step applied)
Suppressed	No

Figure 5.2 Details of Displacement employed on the Workpiece

Tabular Data					
	Steps	Time [s]	<input checked="" type="checkbox"/> X [mm]	<input checked="" type="checkbox"/> Y [°]	<input checked="" type="checkbox"/> Z [mm]
1	1	0.	0.	0.	0.
2	1	1.e-005	= 0.	100.	= 0.
*					

Figure 5.3 Tabular data of the Displacement of the Workpiece

5.1.3 Displacement to the Tool

The tool will be penetrating the workpiece and will be moving in a linear manner for the cutting process to be performed on the workpiece. A linear displacement is given to the tool to move linearly towards the workpiece on its linear axis. For this linear movement of the tool, an axis of the global coordinate system is used. So, a single axis from the global coordinate system is selected for the linear displacement of the tool. For the displacement to

work on the tool, it is important to select the faces one by one instead of selecting the whole body at a time. There are four faces selected for the displacement setting to work on the tool. The end time used for the analysis is 0.00001 s as the process will take a very small time to finish. If we take a large end time, we will miss the calculated solution in between the time step. The linear displacement of the tool is employed on the x-axis of the global coordinate system. At the end time, the linear motion chosen for the analysis is -50 as the tool is going to penetrate the workpiece in that direction. A representation of the boundary condition i.e., displacement employed on the tool is shown in Fig. 5.4.

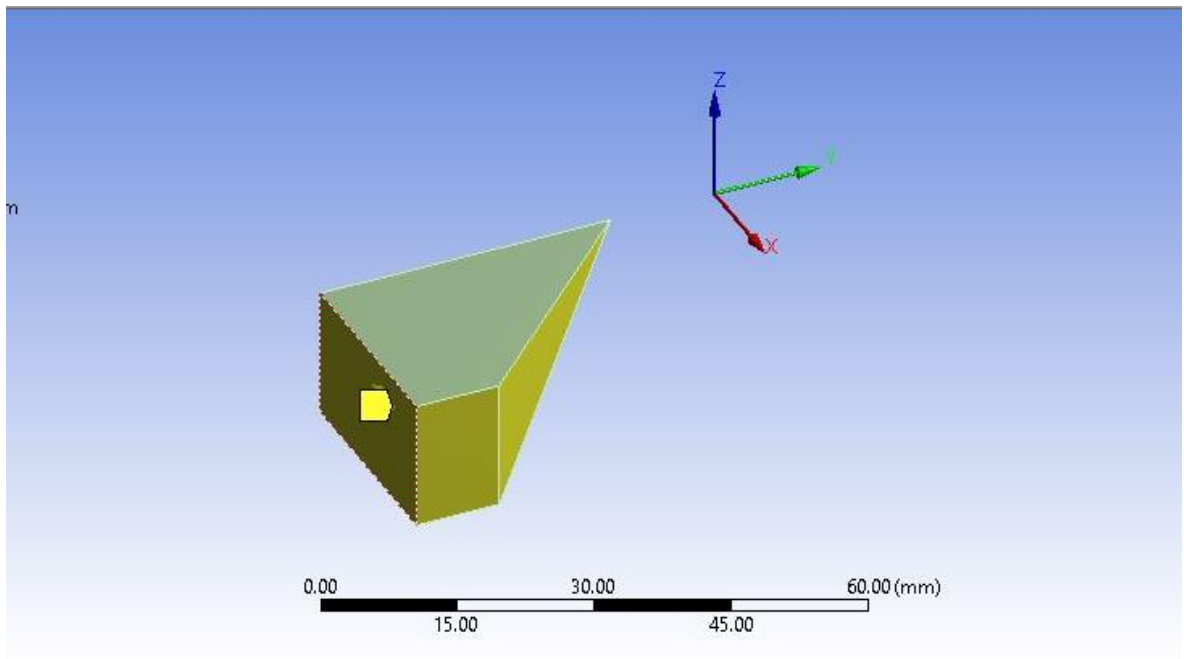


Figure 5.4 Displacement employed on Tool

There are two options available to select the details of the displacement i.e., scope and definition. Scope provides details about the selection of the geometry and the faces chosen for the displacement employed in the turning process. The definition provides the details and the options available for the employment of the displacement to a body, in this case, the tool. The type of displacement is defined by the components of the axes. The coordinate used for the tool is a global coordinate system. The details of the displacement employed on the tool are shown in Fig. 5.5.

The only data remaining about the displacement is the details about the axes where the displacement is taking place. This data is shown in two places, one is in the details with the components and the second one is in the tabular form. In the tabular form, the displacement on the x-axis is shown concerning the time step taken or the end time taken. The table also shows all the data, if multiple displacement point is used in the system. For this thesis, there is only one displacement point is used. The coordinate system shows the data of the axes available to the system in a tabular form which is shown in Fig. 5.6.

[-] Scope	
Scoping Method	Geometry Selection
Geometry	4 Faces
[-] Definition	
Type	Displacement
Define By	Components
Coordinate System	Global Coordinate System
<input type="checkbox"/> X Component	-5. mm (ramped)
<input type="checkbox"/> Y Component	0. mm (ramped)
<input type="checkbox"/> Z Component	0. mm (ramped)

Figure 5.5 Details of Displacement employed on the Tool and the Tool Holder

Tabular Data					
	Steps	Time [s]	<input checked="" type="checkbox"/> X [mm]	<input checked="" type="checkbox"/> Y [mm]	<input checked="" type="checkbox"/> Z [mm]
1	1	0.	0.	0.	0.
2	1	1.e-005	-5.	0.	0.
*					

Figure 5.6 Tabular data of the Displacement of the Tool and the Workpiece

5.2 Analysis Settings

Analysis settings are the settings related to the analysis. These settings control the options settings, time, and other things in an analysis. There are some options available for setting up analysis settings like step controls, solver controls, damping controls, erosion controls, etc. Analysis Setting is the most important part of an analysis and it influences the analysis to its origin the most. So, it is important to choose the correct values for the analysis setting options.

The following sections in this chapter describe all the available properties and settings for the Analysis Settings folder available in an Explicit Dynamics analysis. In addition to detailing each parameter, it is stated if the setting is accessible for 2D studies and whether it is available when the program is restarted and it also applies to 2D and 3D both analyses.

5.2.1 Step Controls

The analysis's completion duration is the needed parameter for step control. This should be set to your best estimate of the time necessary to solve the problem being modeled. Usually, you should let the solver choose its time step size depending on the model's lowest CFL (Courant–Friedrichs–Lewy) condition. The solution's effectiveness can be boosted by using mass scaling methods. Use this tool carefully; excessive mass scaling might lead to a non-physical outcome. At any moment in time, an Explicit Dynamics approach can be begun, halted, and restarted. For instance, an established system that has achieved its End Time may be prolonged to keep reviewing the advancement of the physical processes represented. The Continue from Cycle option allows you to choose which Restart file you want to use to restart the study. Explicit dynamics studies are always completed in a single step. The step control options are shown in Fig. 5.7.

Step Controls	
Number Of Steps	1
Current Step Number	1
End Time	1.e-005
Resume From Cycle	0
Maximum Number of Cycles	1e+05
Maximum Energy Error	0.1
Reference Energy Cycle	0
Initial Time Step	Program Con...
Minimum Time Step	Program Con...
Maximum Time Step	Program Con...
Time Step Safety Factor	0.9
Characteristic Dimension	Diagonals
Automatic Mass Scaling	Yes
Minimum CFL Time Step	1.e-020 s
Maximum Element Scaling	100.
Maximum Part Scaling	5.e-002
Update Frequency	0

Figure 5.7 Step Control Options

5.2.2 Solver Controls

We use these advanced options to modify a variety of solver characteristics, including element formulations and solution velocity limitations. The default settings are useful for a variety of purposes. Only the Explicit Dynamics system may configure density update, minimum velocity, shell inertia update, maximum velocity, the shell thickness update, and radius cutoff settings is an advantage of using solver controls. During the solution, all model variables will be translated to this set of units. In the GUI, the results Solve Units from the analysis will be translated back to the client values standard. This value is always mm, mg, ms for Explicit Dynamics systems. The solver control options are shown in Fig. 5.8.


 Solver Controls	
Solve Units	mm, mg, ms
Beam Solution Type	Bending
Beam Time Step Safety Factor	0.5
Hex Integration Type	Exact
Shell Sublayers	3
Shell Shear Correction Factor	0.8333
Shell BWC Warp Correction	Yes
Shell Thickness Update	Nodal
Tet Integration	Average Nod...
Shell Inertia Update	Recompute
Density Update	Program Con...
Minimum Velocity	1.e-003 mm s...
Maximum Velocity	1.e+013 mm ...
Radius Cutoff	1.e-003
Minimum Strain Rate Cutoff	1.e-010

Figure 5.8 Solver Control Options

5.2.3 Euler Domain Controls

The Euler Domain is defined by three sets of attributes: the length of the entire domain (Domain Length Description), the number of computational cells in the domain (Domain

Resolution Description), and the kind of boundary constraints to be imposed on the domain's borders. The domain size is defined automatically (Domain Size Definition = Program Controlled) or manually (Domain Size Definition = Manual). The size is set by a 3D start location and the domain's X, Y, and Z parameters for both the automated and manual modes. If a body is defined as Eulerian which means the body is defined as a virtual body, the Euler domain frame is shown in the graphical frame when Analysis Settings is chosen in the outline view. The Display Euler Domain setting in the Analysis Settings may be used to regulate its appearance. The Euler domain control options are shown in Fig. 5.9.

Euler Domain Controls	
Domain Size Definition	Program Con...
Display Euler Domain	Yes
Scope	All Bodies
X Scale factor	1.2
Y Scale factor	1.2
Z Scale factor	1.2
Domain Resolution Definition	Total Cells
Total Cells	2.5e+05
Lower X Face	Flow Out
Lower Y Face	Flow Out
Lower Z Face	Flow Out
Upper X Face	Flow Out
Upper Y Face	Flow Out
Upper Z Face	Flow Out
Euler Tracking	By Body

Figure 5.9 Euler Domain Control Options

5.2.4 Damping Controls

Damping is employed in decreased integration components to regulate vibrations following seismic waves and to decrease hourglass modes. These settings enable users to change the dampening and simulation levels utilized in the study. After a dynamic event, elastic waves in the system can be dynamically dampened to create a quasi-static response. For the Flanagan Belytschko option, just one of the Viscous Coefficient or Stiffness Coefficient is utilized for Hourglass Damping. when doing an Explicit Dynamics analysis using the ls-Dyna solver, ls-dyna does not allow for multiple coefficients to be supplied in the hourglass.

Thus, a non-zero coefficient defines whether the damping form is "Flanagan-Belytschko viscous" or "Flanagan-Belytschko stiffness." If both are non-zero, the Stiffness Coefficient is applied. The damping control options are shown in Fig. 5.10.

Damping Controls	
Linear Artificial Viscosity	0.2
Quadratic Artificial Viscosity	1.
Linear Viscosity in Expansion	No
Artificial Viscosity For Shells	Yes
Hourglass Damping	AUTODYN Sta...
Viscous Coefficient	0.1
Static Damping	0.

Figure 5.10 Damping Control Options

5.2.5 Erosion Controls

Erosion is often used in situations like cutting and impact penetration to immediately eliminate excessively deformed pieces from an assessment. Erosion is a numerical method used in an Explicit Dynamics analysis to assist preserve huge time steps and hence achieve solutions at acceptable time scales. There are several ways to start erosion. The default settings will degrade components that have geometric stresses of more than 150 percent.

When modeling hyper elastic materials, the default value should be raised. If a material breakdown characteristic is established in the material used throughout the components and the failure condition is met, the elements will automatically erode. Components with materials that include a damage model will indeed erode if the damage reaches a certain value of 1.0. The erosion control options are shown in Fig. 5.11.

[-] Erosion Controls	
On Geometric Strain Limit	Yes
Geometric Strain Limit	0.258
On Material Failure	Yes
On Minimum Element Time Step	No
Retain Inertia of Eroded Material	Yes

Figure 5.11 Erosion Control Options

5.2.6 Output Controls

Files that contain nodal and element data for contouring and probing outcomes such as deformation, velocity, stress, and strain. Due to the infrequency with which results in files are saved, probe results will offer a filtered temporal history of the results obtained. Restart files, which may be used to continue analysis, should be saved less often than results documents. Tracker data is often kept considerably more often than outcomes or startup data and is thus utilized to generate complete transient data for particular quantities. When doing an implicit to explicit analysis, the Strain Parameters view the property must be set to Yes for a complex implicit analysis since plastic strains are required for accurate findings. The output control options are shown in Fig. 5.12.

[-] Output Controls	
Save Results on	Equally Spac...
Result Number Of Points	200
Save Restart Files on	Equally Spac...
Restart Number Of Points	5
Save Result Tracker Data on	Cycles
Tracker Cycles	1
Output Contact Forces	Off

Figure 5.12 Output Control Options

CHAPTER 6

6 PERFORMING THE EXPERIMENT

6.1 Strategy

The strategy of performing this experiment is to use a computer numerical controlled machine to perform the turning process and to take the force measurements which we use later on to calculate the stresses and the strain involved in the process. First of all, we fixed our workpiece i.e., the circular AA6082-T6 bar to the chuck so that it cannot be moved from its place. The workpiece is now fixed and cannot move from its place, it will only rotate in the circular motion with the chuck. After the workpiece is fixed in its place the tool is to be placed in its place i.e., the tool holder. After placing the tool and the workpiece in their respective places the tool and the workpiece are to be checked that they are fixed properly or not regarding the safety issues and also related to the smooth operation of the machine. The part program is then generated using Siemens Sinumerik 828D CNC machine that comes with version 4.8 of the operating system which will also be used for the performing of the turning process later. The starting and the safety commands of the part program are to be written manually and the cutting cycle is to be substituted with the help of the stock removal cycle of the machine. The Turning process is then performed and the measurements are then taken with a dynamometer. With the help of these experimental results, we will find out the analytical results like stresses, and strains involved in the system. Then these analytical results are to be compared with the FEA results.

6.1.1 Apparatus Used

There are two types of apparatus used in this study of a CNC turning process. The first type of apparatus is a machine for performing the turning process and the other one is a measurement device to measure the parameters in the turning process. The first apparatus i.e., the machine used for the turning process is Siemens Sinumerik 828D which is a computer numerically controlled machine and the second apparatus is a measuring device used for measuring forces and its components are Kistler 9129AA. Both the machines are available at Integral University, Lucknow where the experiment is performed.

6.1.2 CNC Machine Used

To perform the Turning process CNC machine used is Siemens Sinumerik 828D, which is an automatic machine that has many different options for the turning process is available. Siemens is a company that makes CNC (computer numerical control) and Sinumerik is a branch of the Siemens family. The Sinumerik 828D controller, with its distinctive CNC capability, establishes efficiency standards for conventional machining on conventional machines, as well as functionality to effortlessly manage grinding machines. Sinumerik 828d has become even more efficient because of new sinamics drives and semiotics motion control motors. The SINUMERIK 828 CNC's innovation software package allows for a variety of application areas, including vertical and basic horizontal machining centers ideal for mold making – surface and cylindrical grinding types of machinery, and two-channel turning centers with response spindle, focused tools, and Y-axis. Durable hardware design, clever controller design, and superior drive and motor innovation offer the best dynamic responsiveness and precision during milling. Improved software-controlled adjustment capabilities, such as friction, nodding, and cogging torque correction, as well as 3D impact detection in all operation conditions, offer improved surface machining accuracy and machine tool reliability. With Sinumerik Operate, all machining techniques, from basic to complicated, can be managed conveniently and with a consistent "feel and look."

Lightweight and also more complicated machinery with extra axes/spindles and Two machining channels may be created using the various CNC performance versions (SW24x, SW26x, and SW28x). As a result, SINUMERIK 828D controls are indeed precisely tailored to the performance needs of standardized machine ideas for turning (T), milling (M), and grinding (G). Autonomous cells play a vital role in increasing the productivity and flexibility of the manufacturing environment. Using the Run My Robot / Easy Connect interface, robots may be easily linked to manufacturing processes to handle jobs. The machine has a screen and a keyboard attached to it also so, the part program also can be written directly on the machine. The machine and its specifications are shown in Fig.6.1 and Fig. 6.2 respectively.



Figure 6.1 Siemens Sinumerik 828D Machine

INTEGRAL UNIVERSITY	
CNC MACHINE LAB	
CENTRAL WORKSHOP	
TECHNICAL SPECIFICATIONS OF CNC LATHE	
MODEL :	CNC LATHE
DESIGN :	HYTECH
CONTROLLER :	SIEMENS 808
SWING OVER BED :	280 MM
SWING OVER CARRIAGE :	120 MM
CENTER DISTANCE :	300 MM
MAX. TRAVEL :	270 MM
SPINDLE DIA INSIDE :	30 MM
SPINDLE BEARING :	ANGULAR TYPE
THRUST MAX. :	320 KG.
TOOL SIZE :	20X20 MM
SPINDLE MOTOR :	AC - 5.0 HP
WEIGHT APPROX :	950 KG.
INPUT SYSTEM :	METRIC/INCH
INTERPOLATION :	LINEAR & CIRCULAR
MIN. MOVEMENT X&Z :	0.001 MM
FEED RATE X & Z :	3000 MM/MIN
FEED OVERRIDE :	110 %
FLOOR SPACE :	2000 X 1500
HIGHT OF MACHINE :	1200 MM
AXIS DRIVE :	SERVO MOTORS
LUB. PUMP MOTOR :	1/10 HP
SERVO MOTOR :	T - 4 NM

Figure 6.2 Specifications of the Machine

6.1.3 Measuring Device Used

The measuring device used in this study is a type of dynamometer which gives the force and its components during a machining process. The device used in this study for the measurement is Kistler 9129AA. Kistler is renowned for elevated detectors and simple-to-use measuring devices. 150 x 107 mm universal dynamometer has naturally high frequencies. The dynamometer configuration allows for precise detection of highly dynamic forces while ensuring minimum heat effects. A multiphase dynamometer is being used to measure the 3 components of the resulting force vector and the three factors of the resulting moment vector.

The dynamometer is organized into four 3-component force transducers that are sandwiched between both the cover plate and the lateral and medial base plates under heavy loading. A slight temperature inaccuracy is produced due to the detectors' specific installation. Each force sensor has three crystalline crystal discs, one responsive to pressure in the y-direction and the other two to shear force in the x or z directions. The forces are evaluated with almost minimal displacement. The four built-in force detectors' impulses are routed to the 9-pole flange connector. Measurements of many components of force-moment are conceivable. A ground isolator is used to install the four sensors. This almost eliminates grounding loop issues. The Kistler 9129AA employed for measurement in this study is shown in Fig. 6.3.



Figure 6.3 Kistler 9129AA

6.1.4 Part Program Used

The part program is a set of commands that describes the work to be performed on a workpiece in the format needed by a machine running computer numerical control (CNC) software. It is the process of converting a drawing sheet into a program sheet. All the

information that the machine receives is always to be converted into a standardized format. Programming is a method of compiling all of the machining data and translating it into a code that the machine tool's management system can understand.

The initial diameter of the workpiece is 25.5 mm and the length is 150 mm. The final diameter is 8.5 mm and the length is the same as the initial as the turning process only reduces the diameter. The diameter reduction is done up to a length of 50 mm. The part program is half-written and half automatically generated with the help of the machine. The start of the process, the safety commands, and the end of the process are to be written manually and the rest of the program i.e., the cutting cycle is auto-generated by the machine. For the auto-generation of the part program, version 4.8 of the operating system is used in the Siemens Sinumerik 828D CNC machine. The stock removal cycle for the turning process is used to generate the part program for the cutting cycle. For the auto-generation of the part program, we have to give some inputs to the machine like the cutting length, feed rate, etc. With these inputs, the machine will generate a code for the cutting cycle of the workpiece. The input and the parameters given to the stock removal cycle are shown in Fig. 6.4. The machine also shows a simulation of your program which can be seen by giving the parameters of the workpiece. The input parameters are given to the machine and shown in Fig. 6.5.

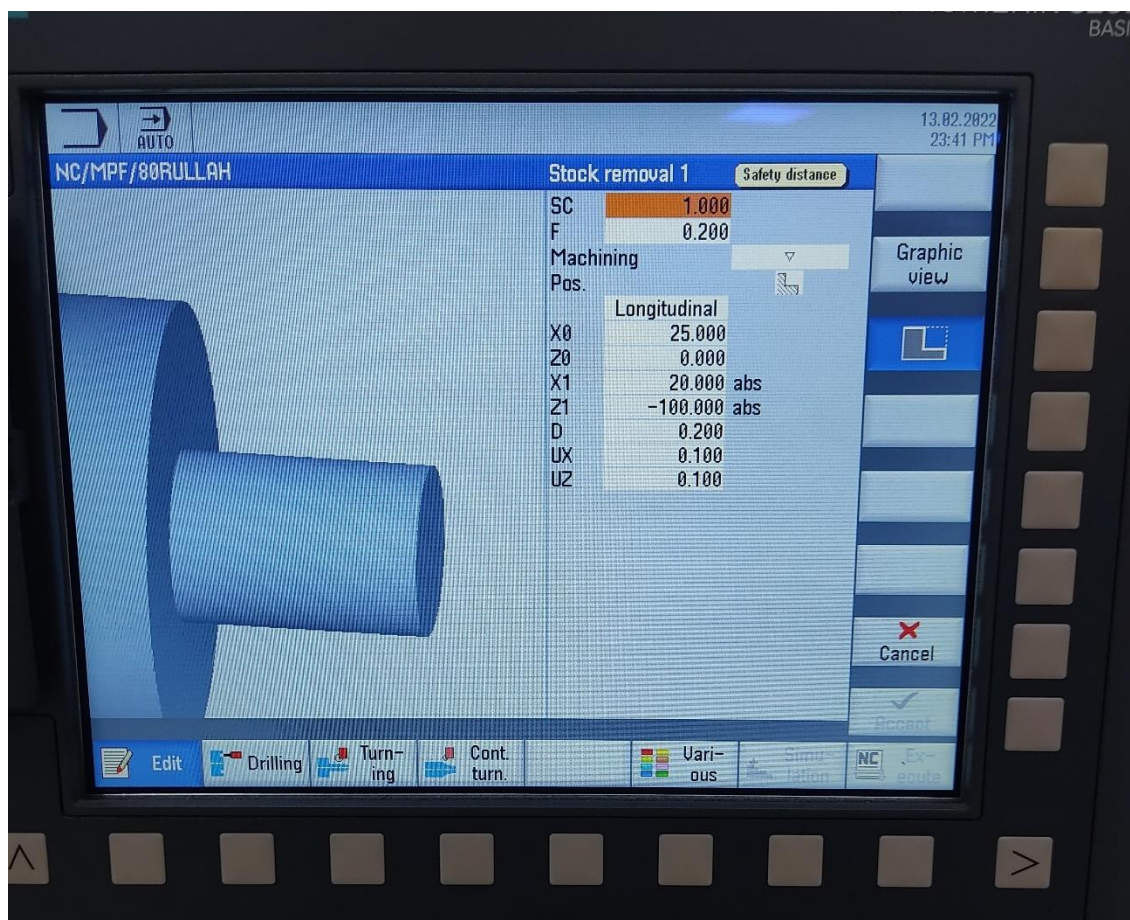


Figure 6.4 Stock Removal Cycle

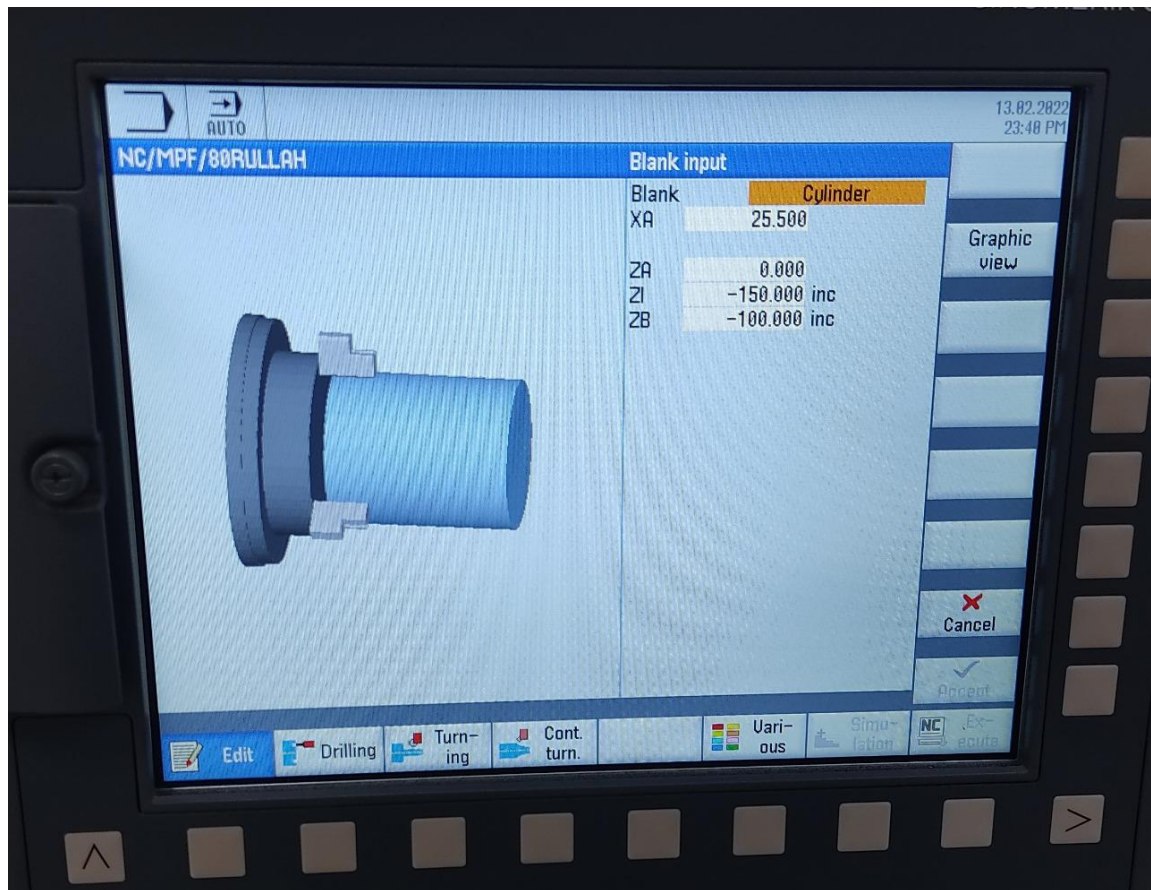


Figure 6.5 Workpiece Parameter Input

After giving all these inputs the part program code for the turning process is completed. The part program contains all the necessary inputs required for performing the turning operation. The part program is

```
WORKPIECE( , , "CYLINDER",0,0,-150,-50,25.5) ||
T="ROUGHING_TOOL"D1 ||
M03 G96 S200 LIMS=1200 ||
G75 X0 Z0 ||
G00 X25.5 Z2 ||
G01 X26 Z0 F0.1 ||
CYCLE951(25.5,0,10,-50,10,-50,1,0.2,0.1,0.1,11,0,0,0,1,0.2,0,2,11100) ||
G75 X0 Z0 ||
M30 ||
||
```

This part program is the input for our turning process. The program in the machine as input is shown in Fig. 6.6. It is clear from the figure that all the required criteria are met for the turning operation to be performed on the machine. There is a line in the figure which shows the time of the turning process but it is the simulated time that came after simulating the part program.

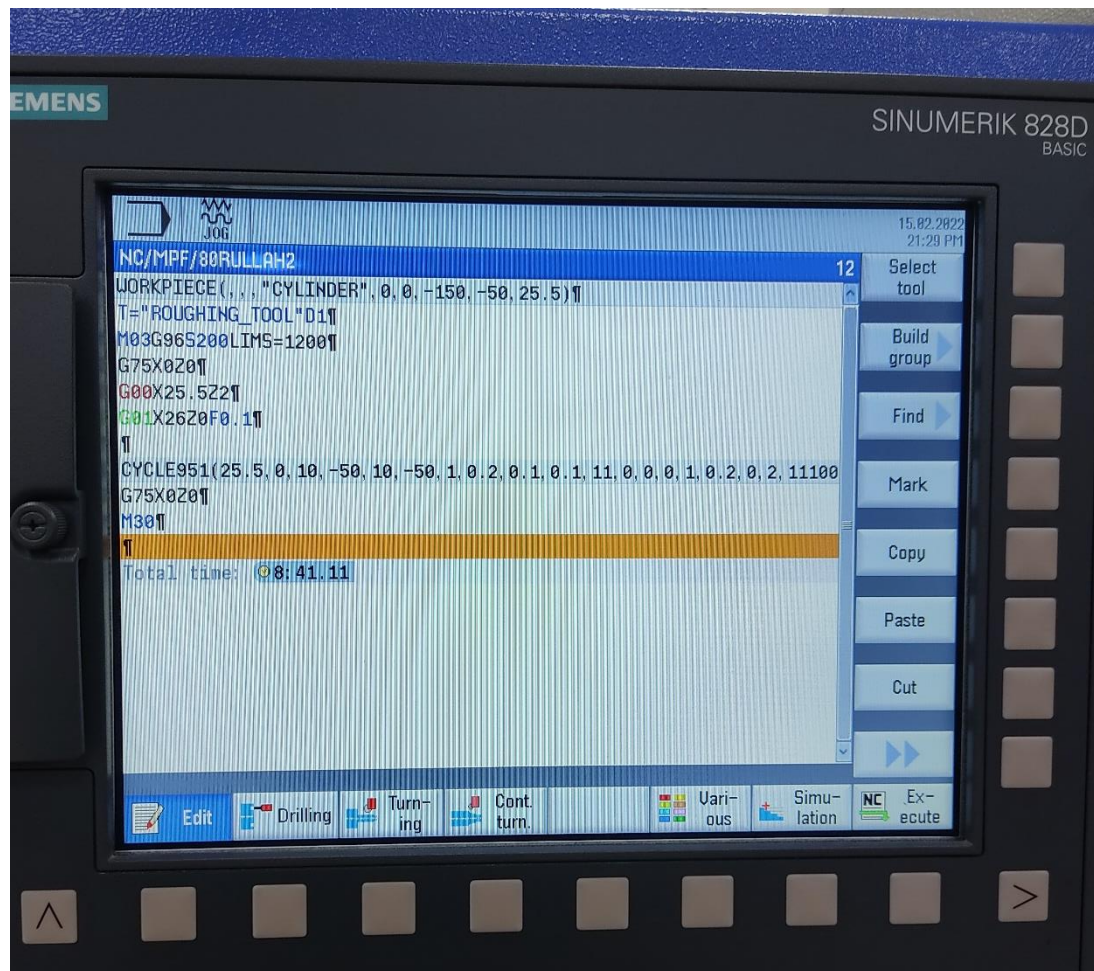


Figure 6.6 Part Program

6.1.5 Performing the Turning Process

Turning is a type of machining that uses a material removal method to make rotatable pieces by removing excess or undesirable material. The turning process necessitates the use of a turning machine or lathe, a workpiece, a fixture, and a cutting tool. The workpiece is a pre-shaped bit of metal that is fixed to the fixture, which is connected to the turning machine and rotated at high speeds. The cutter is normally a single-point cutting tool that is also fastened in the device, while multi-point cutters are used in specific applications. To generate the

required shape, the cutting tool goes into the spinning workpiece and removes material in the form of tiny chips. For the turning process to be performed there are some steps that are involved. First is to fasten the tool and the workpiece to the tool holder and the chuck respectively. Before running the part program, we generated we have to calibrate the machine's coordinate system i.e., we have to give the coordinates to the machine that where will the tool be touching the workpiece. For this calibration, the x-axis and the z-axis is to be feed to the machine. Then the part program is to be run on the machine means to start the machine or the process with the part program which is explained in the earlier section of this chapter. The tool holder and the tool move from its default position towards the workpiece which is also shown in the Fig. 6.7.

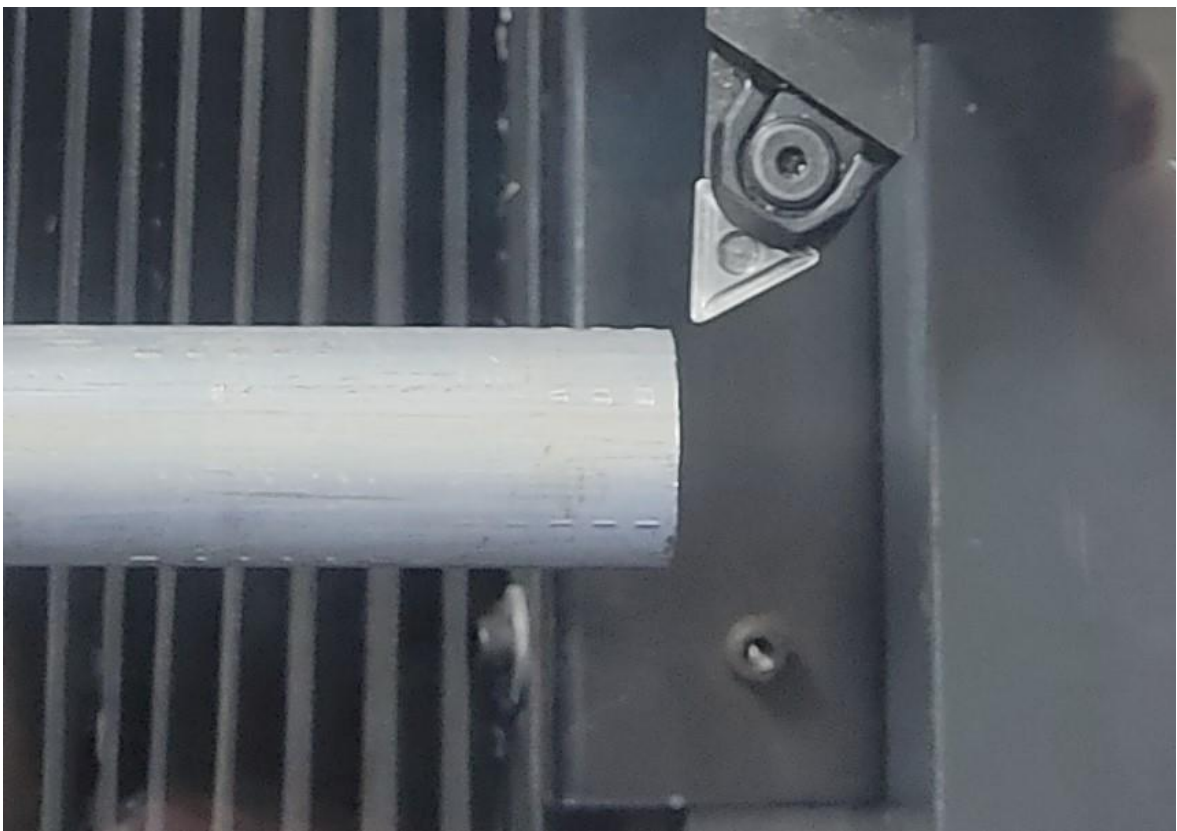


Figure 6.7 Tool moving towards the workpiece

When the tool reaches the position of the tool the cutting action starts or we can also say that the turning process is started. The tool will start cutting the workpiece i.e., reducing the diameter of the workpiece. As the diameter of the workpiece is reduced there is a new layer available underneath every layer that is cut off from the workpiece. This new surface of the workpiece is smoother and brighter related to the first or the outer layer of the workpiece which was cut off in the first cycle of the tool. This surface can easily be seen in Fig. 6.8.

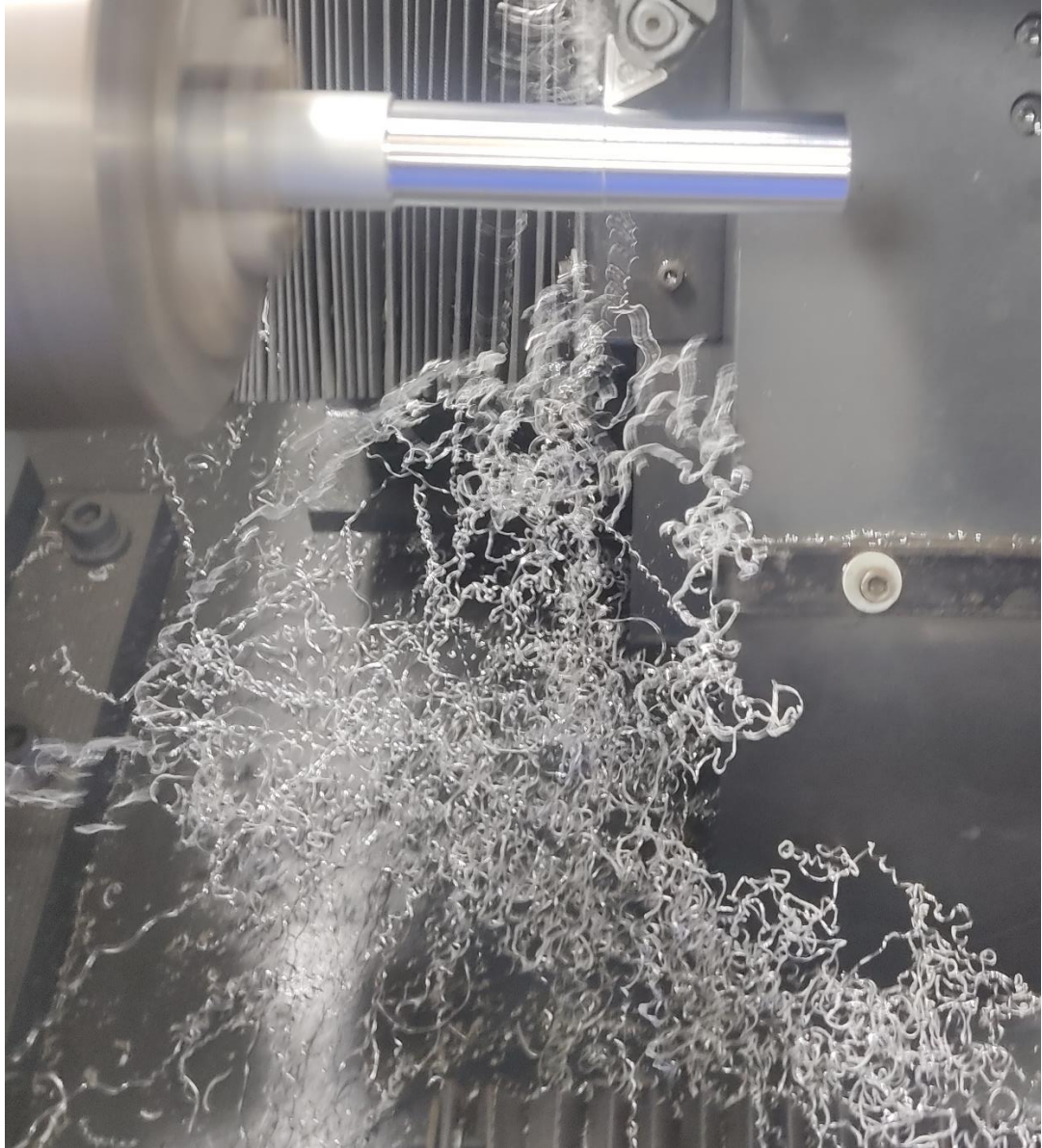


Figure 6.8 Tool Cutting the Workpiece

The tool continuously performs the cutting cycle until we reached the diameter of 8.5 mm from the diameter of 25.5 mm. The tool completes many cycles with a feed of 0.1 mm/rev. and depth of cut as 0.2 mm. After completing all the cycles i.e., when the turning process is completed and the diameter of the workpiece reached a diameter of 8.5 mm the tool stops the cycles and starts to move away from the workpiece and goes to its default position or we can say it as the origin. The tool moves away from the workpiece as shown in Fig. 6.9. When the turning was going on i.e., the cutting cycle was running there were layers of the pieces of the workpiece that was cut away from the workpiece. This layer which is getting cut from the workpiece is called a chip. The chip in this turning is a continuous type of chip as the chips that came out from the workpiece are very long. The chip can also be seen in Fig. 6.8 where the cutting process is going on. The chips cut from the workpiece are shown in Fig. 6.10.



Figure 6.9 Tool Moving away from the Workpiece



Figure 6.10 Chips formed in Turning Process

6.2 Final Product

The final product is the product we get after the conventional machining is carried out on an initial product or else known as Workpiece. This workpiece after the processing and the finishing becomes the end product. This final product is also known as the finished product in the industry as this product has met all its requirements and now it is ready to face the market. In manufacturing, a final product, also known as a finished product, is a product that is ready for sale. An oil industry's finished product, for example, is oil. The producer sells his crops as a finished product once they have gone through the entire growth phase.

In this study, the final product is a bar having the desired diameter of 8.5 mm up to a length of 50 mm and the diameter of 20 mm up to a length of 100 mm. This is the product of our turning process that was carried on earlier. The final product and its measurements are shown in Fig. 6.11 and Fig. 6.12 respectively.

Fig. 6.11 shows the final and the finished product of our study having a diameter of 8.5 mm from the front and 20 mm from the back. The diameter of the final product is measured by a digital vernier caliper which is also shown in Fig. 6.12 withy the diameter of our final product.



Figure 6.11 The Final Product



Figure 6.12 Final Diameter of the Workpiece

CHAPTER 7

7 RESULT & JUSTIFICATION

7.1 FEA Results

Finite Element Analysis (FEA) is the mathematical simulation of any given physical phenomenon using the Finite Element Method (FEM) using Finite element models. Professionals use FEA software to reduce the number of physical prototypes and experimentations, as well as optimize elements during the design process, to facilitate positive goods quickly and at a lower cost. To fully comprehend and accurately measure any physical properties, such as systemic or fluid behavior, thermal transit, vibration, biological cell expansion, and so on, mathematics must be used. Partial Differential Equations are used to characterize the majority of these procedures (PDEs). Nevertheless, for the research to solve such Partial Differential Equations, numerical methods such as Finite Element Analysis were developed over the last several decades. A system of equations is used to characterize both natural and physical phenomena experienced in solid mechanics. These partial differential equations (PDEs) are complex equations that must be answered to calculate relevant structural measurements (such as stresses, strains, and so on) to calculate structural behavior under a specified load.

It is critical to understand that the Finite element method provides only an estimated solution to the issue and is a mathematical approach to obtaining the true result of these partial differential equations. To put it simply, FEA is a numerical model for estimating how a part or assembly will behave or start behaving under certain circumstances. It serves as the foundation for advanced simulators, assisting professionals in identifying weaknesses, areas of strain, and other flaws in their models. The outcomes of an FEA-based simulated world are frequently represented using a color scale that indicates, for example, the stress distribution over the entity. Finite Element Analysis began with incredible potential in modeling a variety of mechanical applications such as aerospace and civil works. Finite Element Method implementations are only now beginning to excel. One of the most promising teams is its implementation of combined issues such as thermo-mechanical, electromagnetics, thermo-chemical, thermo-chemo-mechanical problems altogether, piezoelectric, ferroelectric fluid-structure interaction, as well as other similar topics. The FEA results in this study are taken in the explicit dynamics module of the Ansys software. The analysis of this study took 3 days up to an estimation. We calculated three results for Normal Stress, Shear Stress, and Shear Elastic Strain based on the analysis. These results

show us the final stage up to some seconds of the analysis where the cutting cycle is started and the tool is started penetrating the workpiece.

The analysis of Normal stress concerning the x-axis is shown in Fig. 7.1. The red color in the figure shows the failure effect of the workpiece i.e., from where the chip will start to cut off from the workpiece. After red the color goes from red to orange followed by yellow with following other various colors. The red color shows the maximum value of the normal stress and the blue color shows the minimum amount of the normal stress in the system. The details related to the Normal stress are given in fig 7.1 in the top left corner of the image. The information available at the end of the analysis is the type of the analysis, the unit of the system, the coordinate of the system, the time, the cycle number, and the time and date of the result calculated and taken into account. This result can also be shown in many other ways like line diagrams, pie charts, graph representations, etc. The result shown in the graph representation in this study is a line graph. A line graph is a type of diagram or a graphical representation that is used to display data that changes constantly concerning time. Line graphs are created by connecting numerous points with one or more straight lines. It can also be known as a line chart. The line graph always has two axes, one is known as the x-axis and the other one is known as y- the axis. The line we have on the horizontal axis is referred to as the x-axis and the line we have on the vertical axis is referred to as the y-axis. The line graph studied in this study is plotted in-between time and the normal stress in the system as the analysis is also done concerning time. The line graph shows the relation between the normal stress and the time. The line graph representation of the system is given in Fig. 7.2.

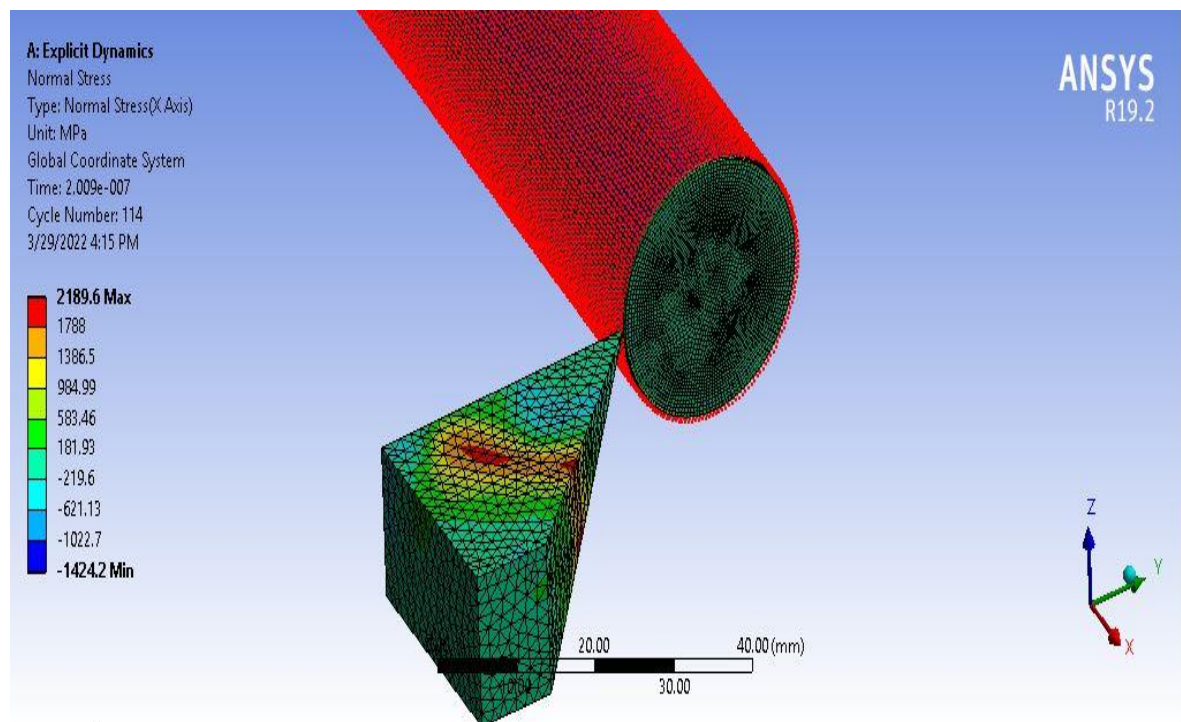


Figure 7.1 Normal Stress Analysis

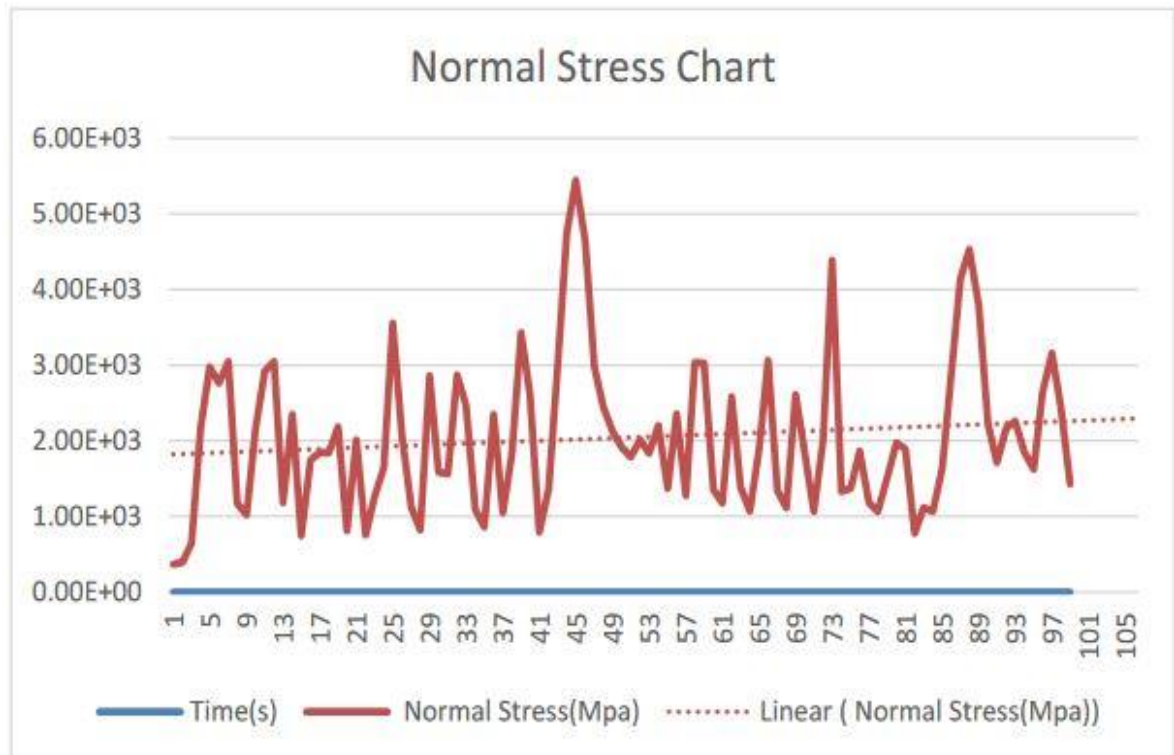


Figure 7.2 Line Graph (Time vs Normal Stress)

The analysis of Shear stress concerning the x-y plane is shown in Fig. 7.3. The red color in the figure shows the failure effect of the workpiece i.e., from where the chip will start to cut off from the workpiece. After red the color goes from red to orange followed by yellow with following other various colors. The red color shows the maximum value of the shear stress and the blue color shows the minimum amount of the shear stress in the system. The details related to the shear stress are given in fig 7.3 in the top left corner of the image. The information available at the end of the analysis is the type of the analysis, the unit of the system, the coordinate of the system, the time, the cycle number, and the time and date of the result calculated and taken into account. This result can also be shown in many other ways like line diagrams, pie charts, graph representations, etc. The result shown in the graph representation in this study is a line graph. A line graph is a type of diagram or a graphical representation that is used to display data that changes constantly concerning time. Line graphs are created by connecting numerous points with one or more straight lines. It can also be known as a line chart. The line graph always has two axes, one is known as the x-axis and the other one is known as y- the axis. The line we have on the horizontal axis is referred to as the x-axis and the line we have on the vertical axis is referred to as the y-axis. The line graph studied in this study is plotted in-between time and the normal stress in the system as the analysis is also done concerning time. The line graph shows the relation between the Shear stress and the time. The line graph representation of the system is given in Fig. 7.4.

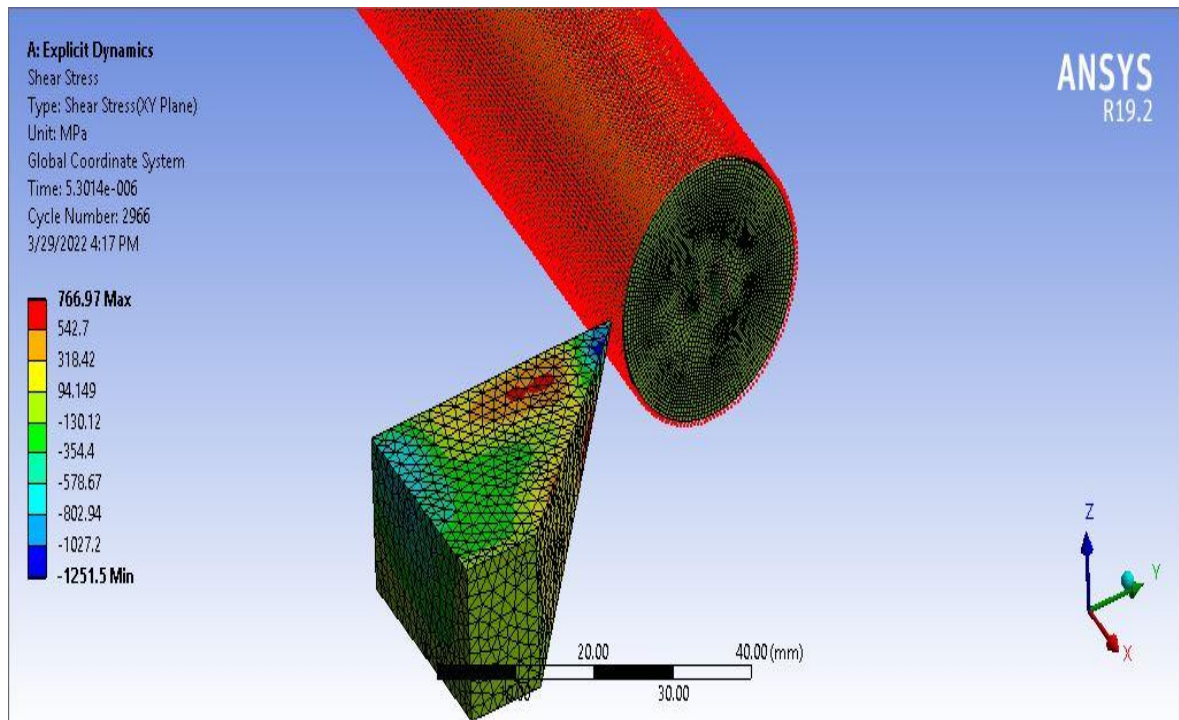


Figure 7.3 Shear Stress Analysis

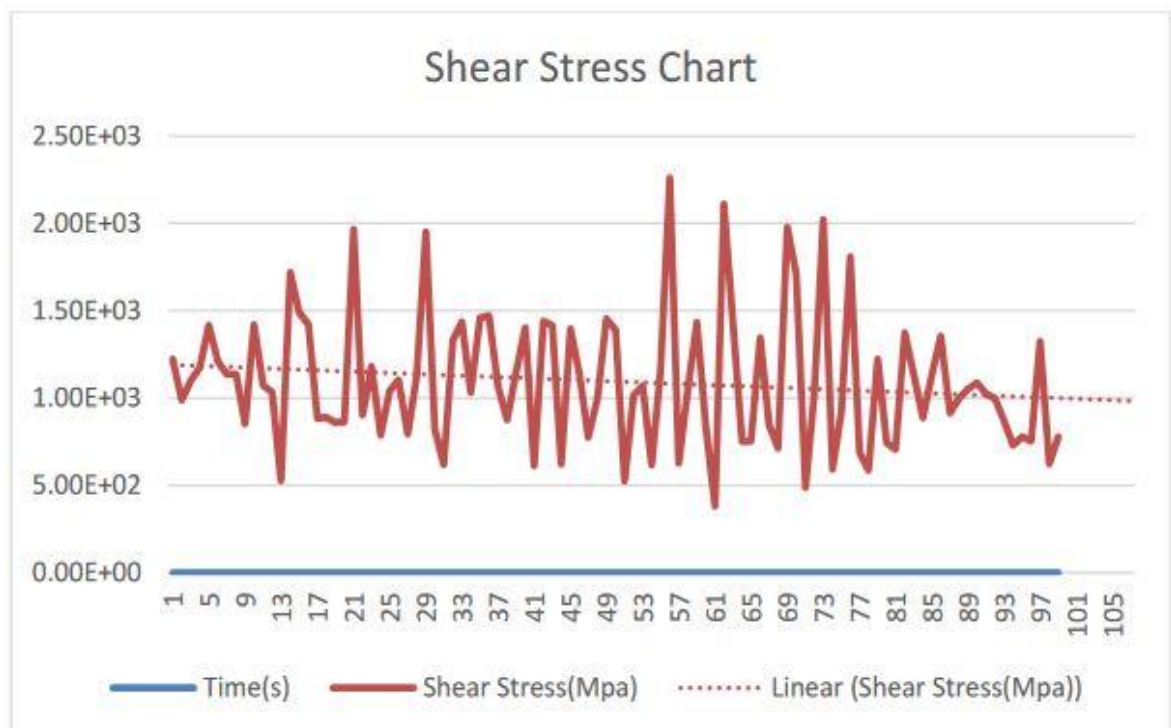


Figure 7.4 Line Graph (Time vs Shear Stress)

The analysis of Shear elastic strain for the x-y plane is shown in Fig. 7.5. The red color in the figure shows the failure effect of the workpiece i.e., from where the chip will start to cut off from the workpiece. After red the color goes from red to orange followed by yellow with following other various colors. The red color shows the maximum value of the shear elastic strain and the blue color shows the minimum amount of the shear elastic strain in the system. The details related to the shear stress are given in fig 7.5 in the top left corner of the image. The information available at the end of the analysis is the type of the analysis, the unit of the system, the coordinate of the system, the time, the cycle number, and the time and date of the result calculated and taken into account. This result can also be shown in many other ways like line diagrams, pie charts, graph representations, etc. The result shown in the graph representation in this study is a line graph. A line graph is a type of diagram or a graphical representation that is used to display data that changes constantly over time. Line graphs are created by connecting numerous points with one or more straight lines. It can also be known as a line chart. The line graph always has two axes, one is known as the x-axis and the other one is known as the y-axis. The line we have on the horizontal axis is referred to as the x-axis and the line we have on the vertical axis is referred to as the y-axis. The line graph studied in this study is plotted in-between time and the normal stress in the system as the analysis is also done concerning time. The line graph shows the relation between the Shear elastic strain and the time. The line graph representation of the system is given in Fig. 7.6.

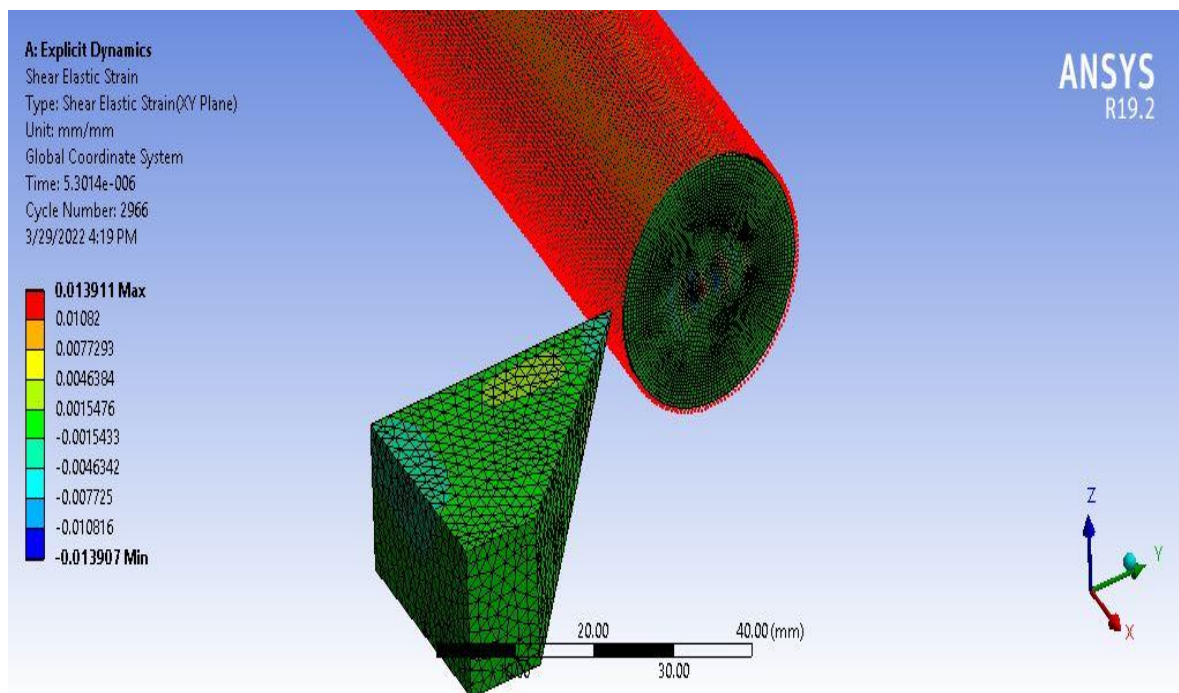


Figure 7.5 Shear Strain Analysis

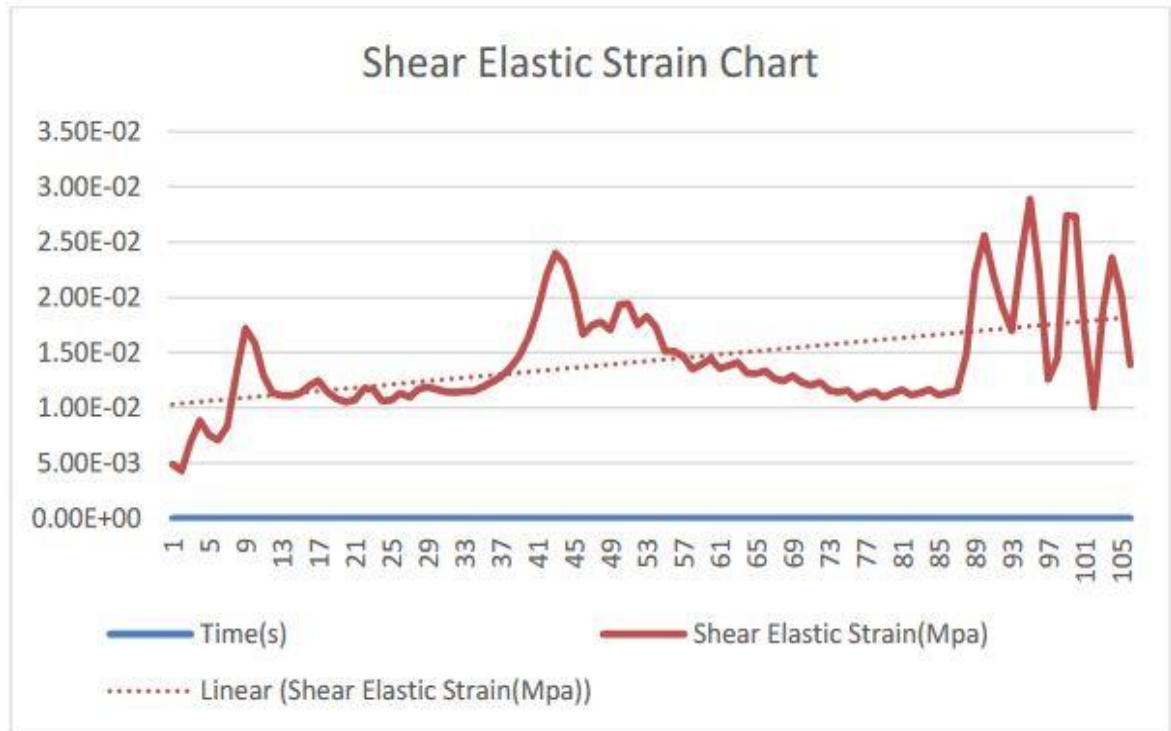


Figure 7.6 Line Graph (Time vs Shear Elastic Strain)

7.2 Experimental Results

As explained in the earlier chapter, the study of the experiment is done on the Siemens Sinumerik 828D CNC machine and the measurement of the forces and the components of the forces are done by a force dynamometer Kistler 9129AA. In physics and technology, experimental information is collected and generated by quantification, testing methods, study research, or experimental layouts. Any data generated in clinical trials is the consequence of a research study. Experimental data can be qualitative or quantitative, depending on the research. In particular, qualitative information is considered more expressive and can be subjective when compared to a constant measuring tool that produces numeric values. Whereas quantitative data is usually collected in an experimentally frequent manner, qualitative information is usually more strongly related to the spectacular significance and is thus up for interpretation by independent researchers. Typically, the goal of a study is to determine the relationships between various potential determinants and the target variable. An experimental unit is the smallest element of an experimental sample that can be selected for treatment. It is critical to select a fair representation set of experimental units that are appropriate for one's research.

The experimental result is shown in the graphical representation in this study. The type of graphical representation used for representing the result is a line graph. A line graph is a type of diagram or a graphical representation that is used to display data that changes constantly time. Line graphs are created by connecting numerous points with one or more straight lines.

It can also be known as a line chart. The line graph always has two axes, one is known as the x-axis and the other one is known as the y-axis. The line we have on the horizontal axis is referred to as the x-axis and the line we have on the vertical axis is referred to as the y-axis. The line graph studied in this study is plotted in-between time and the normal stress in the system as the analysis is also done concerning time. The line graph shows the relation between the component ratio and the time based on the experimental results. The line graph representation of the system is given in Fig. 7.7.

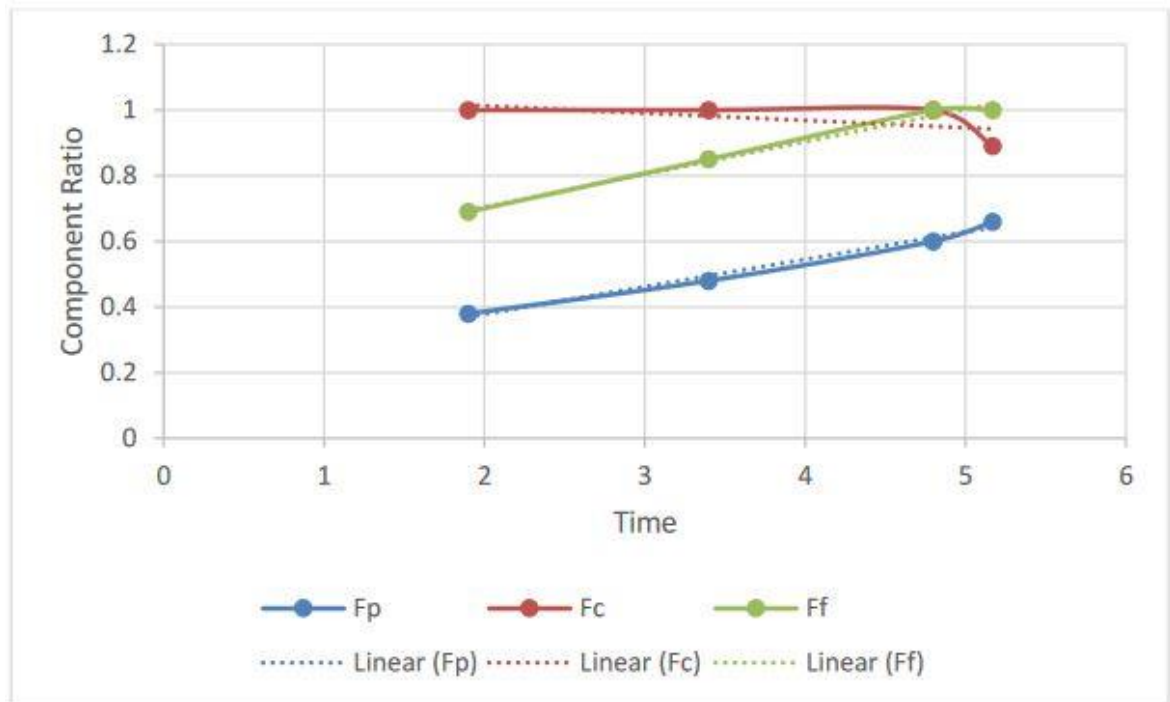


Figure 7.7 Component Ratio vs Time Graph of Results

7.3 Analytical Results

Analytical Results refer to all affiliations, information, variations in results produced by the experiments results or its assessment of FEA Data and/or Experimental Data for the Research or study purposes. Rational series of operational processes, described broadly, used in quantification achievement", e.g., the connections of a given analysis methods with specific stimulation and recognition. Analytical procedure is a set of operational processes that are specifically explained and used in the performance of individual measurement techniques according to several specific implementation. One of most crucial components of any analytical result is its dependability. An analytical result is not really a fixed value; it has two characteristics: error and uncertainty. Each of these parameters' source materials must be identified, and their characteristics must be calculated. All analytical findings are achieved through the use of a suitable measuring methodology. In this study, the analytical

results are calculated by the formulas and conditions related to the cutting conditions based on the experimental results.

The spindle speed in this study is 200 rev./min. with the feed rate of 0.1 mm/rev. and the depth of cut taken in this study is equal to 0.2 mm. With the help of the graph and the experimental results, we have

$$\text{Radial Force Component, } F_r = 0.66 \quad (7.1)$$

$$\text{Cutting Force Component, } F_c = 0.89 \quad (7.2)$$

$$\text{Feed Force Component, } F_f = 1 \quad (7.3)$$

Based on the above values and concerning the experimental results we will now find the analytical values for the Normal Stress, the Shear Stress, and the Shear Strain. Before finding these parameters, we have to find some other parameters like thrust force component, rake angle, Shear angle, etc. The analytical results are shown in this section.

$$\text{Radial Force component, } F_r = F_t \sin \Psi \quad (7.4)$$

$$\text{Thrust Force component, } F_t = \frac{Fr}{\sin \Psi} = \frac{0.66}{\sin 90^\circ} = 0.66 \quad (7.5)$$

We can find the Thrust force component required to find the values which will be compared to the FEA results calculated in the Ansys software. with the values given in the Eqn. (7.1), (7.2), and (7.3). By solving the equation, we get the value of the thrust force component which is 0.66 stated in the Eqn. (7.5).

$$\tan \alpha_b \cos \Psi_s = \tan \alpha_s \sin \Psi_s \quad (7.6)$$

$$\frac{\sin \Psi_s}{\cos \Psi_s} = \frac{\tan \alpha_b}{\tan \alpha_s}$$

$$\tan \Psi_s = \frac{\tan 0}{\tan 5}$$

$$\Psi_s = \tan^{-1} (0) = 0^\circ \quad (7.7)$$

From the equation shown in Eqn. (7.6) we can get the value of the Side cutting edge angle which we will use to find the required values. By solving the equation, we get the value of the Side Cutting edge Angle of the tool which is 0° stated in the Eqn. (7.7).

$$\alpha = \tan^{-1} \left[\frac{\tan \alpha_b \sin \Psi_s + \tan \alpha_s \cos \Psi_s}{\sqrt{1 + (\tan \alpha_b \cos \Psi_s - \tan \alpha_s \sin \Psi_s)^2}} \right] \quad (7.8)$$

$$\alpha = \tan^{-1} \left[\frac{0 + \tan 5 \cos 0}{\sqrt{1 + (0 - \tan 5 \sin 0)^2}} \right]$$

$$\alpha = \tan^{-1} \frac{0.0875}{\sqrt{1}}$$

$$\alpha = 5^\circ \quad (7.9)$$

From the equation shown in Eqn. (7.8), we can find the value of normal rake angle which will be later on used to find the value of shear strain in the system. By solving this equation, we can get the value of the Normal rake angle i.e., 5° stated in the Eqn. (7.9).

$$\text{Cutting Ratio, } r = \frac{t}{t_c} \quad (7.10)$$

$$r = \frac{0.2}{0.22}$$

$$r = 0.909 \quad (7.11)$$

From the equation shown in Eqn. (7.10), we can find the value of the cutting ratio which will be later on used to find the value of the shear angle in the system. By solving this equation, we can get the value of the Cutting Ratio i.e., 0.909 stated in the Eqn. (7.11).

$$\tan \phi = \frac{r \cos \alpha}{1 - r \sin \alpha} \quad (7.12)$$

$$\tan \phi = \frac{0.909 \cos 5}{1 - (0.909 \sin 5)}$$

$$\tan \phi = 0.983$$

$$\phi = \tan^{-1} (0.983)$$

$$\phi = 44.51^\circ \quad (7.13)$$

From the equation shown in Eqn. (7.12), we can find the value of the Shear Angle which will be later on used to find the value of the normal stress, the shear stress, and the shear strain in the system. By solving this equation, we can get the value of the Shear Angle i.e., 44.51° stated in the Eqn. (7.13).

Now, we have all the values required to find out the value of the Normal Stress, the Shear stress, and the Shear Strain. We will use all the values we calculated to calculate the stresses in the system.

$$\text{Normal Stress, } \sigma = \frac{(F_c \sin \phi + F_t \cos \phi) \sin \phi}{bt} \quad (7.14)$$

Putting the values of Eqn. (7.2), Eqn. (7.5) and Eqn. (7.13), we get

$$\sigma = \frac{[0.89 \sin(44.51) - 0.66 \cos(44.51)] \sin(44.51)}{0.75 \times 0.2}$$

$$\sigma = \frac{(0.6239 - 0.47066) 0.7010}{0.15}$$

$$\sigma = 716.14 \text{ MPa} \quad (7.15)$$

From the equation shown in Eqn. (7.14), we found the value of the Normal Stress which is the desired value. By solving this equation, we get the value of the Normal Stress i.e., 716.14 MPa stated in the Eqn. (7.15).

$$\text{Shear Stress, } \tau_s = \frac{(F_c \cos \phi - F_t \sin \phi) \sin \phi}{bt} \quad (7.16)$$

Putting the values of Eqn. (7.2), Eqn. (7.5) and Eqn. (7.13), we get

$$\tau_s = \frac{[0.89 \cos(44.51) - 0.66 \sin(44.51)] \sin(44.51)}{0.75 \times 0.2}$$

$$\tau_s = \frac{(0.6347 - 0.4627) 0.7010}{0.15}$$

$$\tau_s = 803.81 \text{ MPa} \quad (7.17)$$

From the equation shown in Eqn. (7.16), we found the value of the Shear Stress which is the desired value. By solving this equation, we get the value of the Shear Stress i.e., 803.81 MPa stated in the Eqn. (7.17).

$$\text{Shear Strain, } \gamma = \cot \phi + \tan(\phi - \alpha) \quad (7.18)$$

Putting the values of Eqn. (7.9) and Eqn. (7.13), we get

$$\gamma = \frac{1}{\tan(44.51)} + \tan(44.51 - 5)$$

$$\gamma = 0.01725 + 0.01246$$

$$\gamma = 0.0184 \quad (7.19)$$

From the equation shown in Eqn. (7.18), we found the value of the Shear Strain which is the desired value. By solving this equation, we get the value of the Shear Strain i.e., 0.0184 stated in the Eqn. (7.19).

In this section of chapter 7, we have seen the analytical results and the values of the stresses and strains in the system. The value of normal stress, the shear stress, and the shear strain are the most important values which will be considered when the comparison between the analytical and the finite element analysis results are done. The percentage error is then calculated for the conclusion of this study.

CHAPTER 8

8 CONCLUSION & FUTURE WORK

8.1 Conclusion

In this thesis, the analysis of the CNC turning process of an aluminum alloy i.e., AA6082-T6 is done successfully. For this analysis, the FEA and the analytical results are carried out. Then the finite element analysis results are compared with the analytical results to find out the percentage error between both the results we got. The percentage error is the difference between the measured value and the true value in comparison with the original value. In other words, the relative error magnified by 100 equals the percent error. The approximation of the errors in a system is also called the percentage error. There are three values of which we have to find out the percentage errors. The first value is Normal stress, the second value is shear stress and the last or the third value is the shear strain. The results and the values are shown in the previous chapter and all the calculation of the stresses and the strains is also done in the previous chapter. The percentage error we get for the Normal stress is -67.3%. The negative mark depicts that the FEA result value is very small about the analytical value that we calculated. The percentage error for the value of Normal stress is too high because the software shows us the stress from the starting point up to the end time given for the analysis and the Normal stress, we got is the value from the starting point up to a certain point in time in relation with the force components. The percentage error value of second stress i.e., shear stress is 4.80%. This percentage error value is very low and depicts that our FEA result value is very near to the analytical value that we calculated based on the experimental results. The percentage error of the third value or the last value i.e., shear strain is 32.27%. This percentage error value is respectively low and depicts that our FEA result value is partially near to the analytical value that we calculated based on the experimental results.

8.2 Future Work

For future research, several topics are considered to expand the present research work. To create the FEA model for the whole CNC system, certain factors should be considered including CNC machine specifications and the accuracy of the machine. The study was done on a circular aluminum alloy which can be replaced with a different shape of alloy with or without the use of the lubrication or chip cutters in the CNC system.

There is a set of cutting parameters used in this study changing them will also increase or decrease the productivity of the process. So, cutting parameters can be changed for better performance. The optimization can be done of the CNC turning process for the aluminum alloy AA6082-T6 workpiece. Aluminum alloys are the most usable material in the industry after steel for CNC machining. So, further analysis and the optimization of the CNC machining can be done.

Because FEA simulation takes a long time, a better meshing method or options for time reduction, or time efficiency, must be researched. More simulation studies with various types of tools and their cutting parameter ranges are required.

REFERENCES

- Dr. Vijay Kumar M, Kiran Kumar B.J, Rudresha N,2018.” Optimization of Machining Parameters in CNC Turning of Stainless Steel (EN19) by TAGUCHI’S Orthogonal Array Experiments”, ICMMM-2017, Materials Today: Proceedings 5 11395–11407.
- R.K.Bharilya, Ritesh Malgaya, Lakhan Patidar, R.k. Gurjar, Dr.A.K.Jha,2015. ” Study of Optimised process parameters in turning operation through Force Dynamometer on CNC Machine”, Materials Today: Proceedings 2-2300-2305.
- Magdum Vikas B., 2013.” Evolution and Optimization Parameter for Turning-En8 steel”, International Journal Engineering Trends and Technology Volume 4 Issue 5 May 2013 pp 1564-1568.
- Mayur Verma,Sharad K. Pradhan,2019.”Experimental and Numerical investigations in CNC turning for different combinations of tool inserts and workpiece material”, Materials Today: Proceedings, <https://doi.org/10.1016/j.matpr.2019.12.193>.
- S.P. Palaniappan, K. Muthukumar, R.V. Sabariraj, S.Dinesh Kumar, T.Sathish,2019.“CNC turning process parameters optimization on Aluminium 6082 alloy by using Taguchi and ANOVA”, Materials Today: Proceedings, <https://doi.org/10.1016/j.matpr.2019.10.053>.
- N. Satheesh Kumar, Ajay Shetty, Ashay Shetty, Ananth K, Harsha Shetty,2012.” Effect of Spindle Speed and feed rate on surface roughness of Carbon Steels in CNC turning”, Procedia Engineering 38 691-697.
- A. Saravankumar, S.C. Karthikeyan, B. Dhamotharan, V. Gokul kumar,2018.” Optimization of CNC Turning Parameters on Aluminum Alloy 6063 using Taguchi Robust Design” materials today: Proceedings volume 5, issue 2 part 2, pages 8290-8298.
- S.K. Saini, S.K. Pradhan,2014.” Optimization of multi-objective response during CNC turning using Taguchi-fuzzy application”, Proc. Eng.97141-149.
- P. Gupta, Bhagat Singh,2021. “Exploration of tool chatter in CNC turning using a new ensemble approach”, materials today: Proceedings volume 43, part 1, pages 640-645.
- D. Umbrello, R. M’Saoubi, J.C. Outeiro,2007.” The influence of Johnson Cook material constants on finite element simulation of machining of AISI 316L steel”,Int. J.Mach. Tools Manuf. 47(3-4)462-470.
- Hussani T.M. EL,2010.” Cutting Parameter optimization when machining different materials”,Material and Manufacturing pp 1101-1114.
- M.Sadílek, J.Dubský, Z.Sadílková, Z.Poruba,2015.” Cutting forces during turning with variable depth of cut” Perspectives in Science, <http://dx.doi.org/10.1016/j.pisc.2015.11.055>.
- Cep, R, et al., 2013.” Experimental testing of cutting inserts cutting ability”, 2013 Teh. Vjesn. /Tech. Gaz. 20 (1), 21—26, ISSN 1330-3651.

Hatala, M., 2007. "Simulation of Technological Process", 1st ed. FVT TU, Prešov, ISBN 978- 80-8073-756-6, pp. 85.

Mohanraj Murugesan, Dong Won Jung, 2019. "Johnson Cook Material and Failure Model Parameters Estimation of AISI-1045 Medium Carbon Steel for Metal Forming Applications", *Materials*, 12, 609; doi:10.3390/ma12040609.

M.Hanief, M.F.Wani, M.S.Charoo, 2016. "Modeling and prediction of cutting forces during the turning of red brass (C23000) using ANN and regression analysis", *Eng. Sci. Tech., Int. J.*, <http://dx.doi.org/10.1016/j.jestch.2016.10.019>.

T. Dorlin, F. Guillaume, J.P. Costes, 2015. "Analysis and modeling of the contact radius effect on the cutting forces in cylindrical and face turning of Ti6Al4V titanium alloy", *Procedia CIRP* 31-185–190.

J. Xie, M.J. Luo, K.K. Wu, L.F. Yang, D.H. Li, 2013. "Experimental study on cutting temperature and cutting force in dry turning of titanium alloy using micro-grooved tool", *Int. J. Mach. Tools Manuf.* 73, 25–36.

A. Pramanik, L.C. Zhang, J. Arsecularatne, 2006. "Prediction of cutting forces in machining of metal matrix composites", *Int. J. Mach. Tools Manuf.* 46 (14) 1795–1803.

Byrne G., Dornfeld D., Inasaki I., Ketteler Konig G. W. and Teti R. 1995. "Tool condition monitoring (TCM)—the statue of research and industrial application," *Ann. b CIRP*, Vol. 44, No. 2, pp. 541–567.

Thamizhmanii S, Saparudin S and Hasan S, 2007. "Analyses of surface roughness by turning process using Taguchi method", *Journal of Achievements in Materials and Manufacturing engineering*, 20(1-2), 503-506.

Magdum V B, Vinayak R. Naik, 2013. "Evaluation and Optimization of Machining Parameter for turning of EN 8 steel", *International Journal of Engineering Trends and Technology*, 4(5), 1664-1668.

Yadav U P, Narang D and Pankaj S A, 2012. "Experimental Investigation and Optimization of Machining Parameters for Surface Roughness in CNC Turning by Taguchi Method", *International Journal of Engineering Research and Applications*, 2, 2060-2065.

A. Zerti, M.A. Yallese, I. Meddour, S. Belhadi, A. Haddad, T. Mabrouki, 2019. "Modeling and multi-objective optimization for minimizing surface roughness, cutting force, and power, and maximizing productivity for tempered stainless steel AISI 420 in turning operations", *Int. J. Adv. Manuf. Technol.* 102 135–157, <https://doi.org/10.1007/s00170-018-2984-8>.

M.D. Sharma, R. Sehgal, 2016. "Modelling of machining process while turning tool steel with CBN tool", *Arabian J. Sci. Eng.* 41 1657–1678, <https://doi.org/10.1007/s13369-015-1864-x>

W. Jomaa, O. Mechri, J. Lévesque, V. Songmene, P. Bocher, A. Gakwaya, 2017. "Finite element simulation and analysis of serrated chip formation during high-speed machining of AA7075–T651 alloy", *J. Manuf. Processes* 26 446–458, <https://doi.org/10.1016/J.JMAPRO.2017.02.015>.

N. Senthilkumar, T. Tamizharasan, 2014. "Effect of tool geometry in turning AISI 1045 steel: experimental investigation and FEM analysis", *Arabian J. Sci. Eng.* 39 4963–4975, <https://doi.org/10.1007/s13369-014-1054-2>

- V. Vijayaraghavan, A. Garg, L. Gao, R. Vijayaraghavan, G. Lu, 2016. "A finite element-based data analytics approach for modeling turning process of Inconel 718 alloys", *J. Cleaner Prod.* 137 1619–1627, <https://doi.org/10.1016/j.jclepro.2016.04.010>.
- K. Gok, 2015. "Development of three-dimensional finite element model to calculate the turning processing parameters in turning operations", *Measurement* 75 57–68, <https://doi.org/10.1016/J.MEASUREMENT.2015.07.034>.
- Kok, M., 2011. "Modeling and assessment of some factors that influence surface roughness for the machining of particle reinforced metal matrix composites", *Arab. J. Sci. Eng.* 36(7), 1347–1365.
- Santha Kumari, K.V., Jana, D.R., Kumar, A., 2010. "Effects of tool setting on tool cutting angle on turning operation", *ARPN J. Eng. Appl. Sci.* 18, 27–31.
- Harish Kumar, Mohd. Abbas, Dr. Aas Mohammad, H. Zakir Jafri, 2013. "Optimization of cutting parameters in CNC Turning", *International Journal of Engineering Research and Applications*, vol. 3, Issue 3, pp. 331-334.
- Hardeep Sing, Simranjeet Sing, Shiva Kumar Sharma, 2014. "Optimization of machining parameter for turning of EN 16 steel", *International journal of engineering and technology E-ISSN 2277-4106 VOL 4*.
- Harshimran Shingh Sodhi, Harjot Shingh, 2013. "Parametric Analysis of copper for cutting processes using turning operations based on Taguchi method", *IJRMET VOL 3*.
- T. Sathish, 2019. "Experimental investigation of machined hole and optimization of machining parameters using electrochemical machining", <https://doi.org/10.1016/j.jmrt.2019.07.046>.
- A.J. Shih, H.T.Y. Yang, 1993. "Experimental and finite element predictions of residual stresses due to orthogonal metal cutting", *Int. J. Numer. Meth. Eng.* 36 (9) 1487–1507.
- R.C. Miroslav, D.C. Predrag, J.C. Predrag, 2017. "Experimental Determination of Cutting Force by Longitudinal Turning of C60E Steel", vol. 2, no. August pp. 113–119.
- T. Özel, T. Altan, 2000. "Determination of workpiece flow stress and friction at the chip-tool contact for high-speed cutting", *Int. J. Mach. Tools Manuf.* 40 (1) 133–152.
- Bagaber SA, Yusoff AR, 2017. "multi-objective optimization of cutting parameters to minimize power consumption in dry turning of stainless steel 316", *J Clean Prod* 157:30–46.
- Camposeco-Negrete C, 2013. "Optimization of cutting parameters for minimizing energy consumption in turning of AISI 6061 T6 using Taguchi methodology and ANOVA", *J Clean Prod* 53:195–20.
- Chabbi A, Yallese MA, Nouioua M, Meddour I, Mabrouki T, Girardin F., 2017. "Modeling and optimization of turning process parameters during the cutting of polymer (POM C) based on RSM, ANN, and DF methods", *Int J Adv Manuf Technol* 91:2267–2290.
- Qu S, Zhao J, Wang T., 2017. "Experimental study and machining parameter optimization in milling thin-walled plates based on NSGA-II", *Int J Adv Manuf Technol* 89(5–8):2399–2409.
- Korkmaz ME, Günay M., 2018. "Finite element modelling of cutting forces and power consumption in turning of AISI 420 martensitic stainless steel", *Arab J Sci Eng*:1–8.

Lalwani DI, Mehta NK, Jain PK.,2008."Experimental investigations of cutting parameters influence on cutting forces and surface roughness in finish hard turning of MDN250 steel", J Mater Process. Technol 206:167–179.

Hualong Xie, Huimin Guo, Qingbao Wang, YongXian Liu,2012."The Spindle Structural Optimization Design of HTC3250µm NC Machine Tool Based on ANSYS", Advanced Materials Research Vols. 457-458 (2012) pp 60-64.

Zanhui Shu, Qiushi Han,2012."Dynamic Analysis Based On ANSYS of Turning and Grinding Compound Machine Spindle Box",Advanced Materials Research Vols. 433-440 (2012) pp 524-529.

Doru Bardac, Constantin Dogariu,2014."Finite Element Analysis for Static Behaviour of the CNC Turning Machine Spindle", Applied Mechanics and Materials Vol. 555 (2014) pp 555-560.

List of Publications

My paper entitled “**COMPARISON BETWEEN AUTOMATED GENERATION OF NC PART PROGRAM FOR TURNING PROCESS**” is Published under International Conference on Industrial and Production Engineering (ICIPE) organized by the South Asian Research Center (SARC) (ISO 9001:2008 Certified) <https://digitalxplore.org/proceeding.php?pid=1416>.

My paper entitled “**MODELLING & ANALYSIS OF CNC TURNING PROCESS USING ANSYS SOFTWARE**” is Published under Dogo Rangsang Research Journal UGC Care Group I Journal ISSN: 2347-7180 Vol-09 Issue-01 No. 01: 2022 https://journal-dogorangsang.in/no_1_Online_22.html.

My paper entitled “**ANALYSIS OF CNC TURNING PROCESS USING ANSYS SOFTWARE**” is presented in the International Conference on Processing and Characterization of Materials (ICPCM –22) organized by SSN College of Engineering.

My paper entitled “**ANALYSIS OF CNC TURNING PROCESS OF AA6082-T6 USING ANSYS SOFTWARE**” is accepted and presented in the “International Conference on Advances in Mechanical Engineering-2022” (ICAME-2022) organized by the Department of Mechanical Engineering G H Raisoni College of Engineering, Nagpur, India and is in the process of publication.

ORIGINALITY REPORT

13%

SIMILARITY INDEX

9%

INTERNET SOURCES

5%

PUBLICATIONS

%

STUDENT PAPERS

PRIMARY SOURCES

1

idoc.pub

Internet Source

2%

2

spectrum.library.concordia.ca

Internet Source

2%

3

en.wikipedia.org

Internet Source

1%

4

Mayur Verma, Sharad K. Pradhan.

"Experimental and numerical investigations in
CNC turning for different combinations of tool
inserts and workpiece material", Materials
Today: Proceedings, 2020

Publication

1%

5

orange.engr.ucdavis.edu

Internet Source

<1%

6

"Key Topics in Surgical Research and
Methodology", Springer Science and Business
Media LLC, 2010

Publication

<1%

7

www.simscale.com

Internet Source

<1%

8	cf.d.ninja Internet Source	<1 %
9	"Handbook of Manufacturing Engineering and Technology", Springer Science and Business Media LLC, 2015 Publication	<1 %
10	"Advances in Forming, Machining and Automation", Springer Science and Business Media LLC, 2019 Publication	<1 %
11	www.mechanicalthink.com Internet Source	<1 %
12	R.K. Bhariya, Ritesh Malgaya, Lakhan Patidar, R.K. Gurjar, A.K. Jha. "Study of Optimised Process Parameters in Turning Operation Through Force Dynamometer on CNC Machine", Materials Today: Proceedings, 2015 Publication	<1 %
13	ijcert.org Internet Source	<1 %
14	Cheung, Y K, and K W Chau. "NONLINEAR FINITE ELEMENT ANALYSIS OF REINFORCED CONCRETE FRAME UNDER DIFFERENT LATERAL LOADING PATTERNS", Tall Buildings, 2005. Publication	<1 %

15	Alexandra-Maria Aluței, Emőke Szelitzky, Dan Mândru. "Transient Thermal State of an Active Braille Matrix with Incorporated Thermal Actuators by Means of Finite Element Method", Assistive Technology, 2013 Publication	<1 %
16	www.freepatentsonline.com Internet Source	<1 %
17	www.technia.co.uk Internet Source	<1 %
18	epdf.pub Internet Source	<1 %
19	Shaw, Milton C.. "Metal Cutting Principles", Oxford University Press Publication	<1 %
20	app.aws.org Internet Source	<1 %
21	dergipark.Org.Tr Internet Source	<1 %
22	www.iosrjournals.org Internet Source	<1 %
23	www.mecheng.osu.edu Internet Source	<1 %
24	Udupikrishna Joshi, Manju Kurakar. "Comparison of Stability of Fracture Segments	<1 %

in Mandible Fracture Treated with Different Designs of Mini-Plates Using FEM Analysis", Journal of Maxillofacial and Oral Surgery, 2013

Publication

25	scholarbank.nus.edu.sg	<1 %
	Internet Source	

26	Feng Fu. "Design and Analysis of Complex Structures", Elsevier BV, 2018	<1 %
	Publication	

27	research.library.mun.ca	<1 %
	Internet Source	

28	starjournal.org	<1 %
	Internet Source	

29	R. Bedira, A. Gharsallah, A. Gharbi, H. Baudrand. "An Iterative Process Based on the Concept of Waves for Electromagnetic Scattering Problems", Electromagnetics, 2010	<1 %
	Publication	

30	theses.lib.polyu.edu.hk	<1 %
	Internet Source	

31	www.rampfesthudson.com	<1 %
	Internet Source	

32	Gang Wang, Hao-Yu Yang. "Extraction of Thermos Cup Contour Based on Optimized Edge Feature and Line Detection", 2020 International Conference on Intelligent	<1 %
----	--	------

Transportation, Big Data & Smart City (ICITBS), 2020

Publication

-
- | | | |
|---|--|----------------|
| <div style="background-color: #800080; color: white; display: inline-block; width: 40px; height: 40px; text-align: center; line-height: 40px;">33</div> | <p>O. Yu. Erenkov, A. G. Ivakhnenko, M. V. Radchenko. "Oscillatory Process of Production Systems during Turning of Caprolon Blanks", Chemical and Petroleum Engineering, 2013</p> <p>Publication</p> | <p><1 %</p> |
|---|--|----------------|
-
- | | | |
|---|--|----------------|
| <div style="background-color: #008000; color: white; display: inline-block; width: 40px; height: 40px; text-align: center; line-height: 40px;">34</div> | <p>www.science.gov</p> <p>Internet Source</p> | <p><1 %</p> |
|---|--|----------------|
-
- | | | |
|---|--|----------------|
| <div style="background-color: #000080; color: white; display: inline-block; width: 40px; height: 40px; text-align: center; line-height: 40px;">35</div> | <p>dspace.lboro.ac.uk</p> <p>Internet Source</p> | <p><1 %</p> |
|---|--|----------------|
-
- | | | |
|---|--|----------------|
| <div style="background-color: #000080; color: white; display: inline-block; width: 40px; height: 40px; text-align: center; line-height: 40px;">36</div> | <p>publications.lib.chalmers.se</p> <p>Internet Source</p> | <p><1 %</p> |
|---|--|----------------|
-
- | | | |
|---|--|----------------|
| <div style="background-color: #ff0000; color: white; display: inline-block; width: 40px; height: 40px; text-align: center; line-height: 40px;">37</div> | <p>www.ijert.org</p> <p>Internet Source</p> | <p><1 %</p> |
|---|--|----------------|
-
- | | | |
|---|--|----------------|
| <div style="background-color: #ff00ff; color: white; display: inline-block; width: 40px; height: 40px; text-align: center; line-height: 40px;">38</div> | <p>Nguyen Lam Khanh, Nguyen Van Cuong. "Chapter 67 Multiple Criteria Decision Making When Turning by Taguchi-Vikor Method", Springer Science and Business Media LLC, 2022</p> <p>Publication</p> | <p><1 %</p> |
|---|--|----------------|
-
- | | | |
|---|--|----------------|
| <div style="background-color: #800080; color: white; display: inline-block; width: 40px; height: 40px; text-align: center; line-height: 40px;">39</div> | <p>repository.dl.itc.u-tokyo.ac.jp</p> <p>Internet Source</p> | <p><1 %</p> |
|---|--|----------------|
-



BABU BANARASI DAS UNIVERSITY, LUCKNOW
CERTIFICATE OF FINAL THESIS SUBMISSION

1. Name:

2. Enrollment No.:

3. Thesis title:

.....

.....

4. Degree for which the thesis is submitted:

5. School (of the University to which the thesis is submitted):
.....

6. Thesis Preparation Guide was referred to for preparing the thesis. ☐ YES ☐ NO

7. Specifications regarding thesis format have been closely followed. ☐ YES ☐ NO

8. The contents of the thesis have been organized based on the Guidelines. ☐ YES ☐ NO

9. The thesis has been prepared without resorting to plagiarism. ☐ YES ☐ NO

10. All sources used have been cited appropriately. ☐ YES ☐ NO

11. The thesis has not been submitted elsewhere for a degree. ☐ YES ☐ NO

12. All the corrections have been incorporated. ☐ YES ☐ NO

13. Submitted 4 spiral bound copies plus one CD. ☐ YES ☐ NO

(Signature of the Candidate)

Name:.....

Roll No.:.....

Enrollment No: